Acta Biomaterialia 139 (2022) 204–217

Contents lists available at ScienceDirect

Acta Biomaterialia

journal homepage: www.elsevier.com/locate/actbio

Full length article

Electrical stimulation of titanium to promote stem cell orientation, elongation and osteogenesis☆

Juan Shong Khaw[a], Ruikang Xue[a], Nigel J. Cassidy[b], Sarah H. Cartmell[a,*]

[a] The Henry Royce Institute, Royce Hub Building, The University of Manchester, Manchester M13 9PL, UK
[b] Civil Engineering, University of Birmingham, Edgbaston, Birmingham B15 2TT, UK

ARTICLE INFO

Article history:
Received 27 February 2021
Revised 6 July 2021
Accepted 6 August 2021
Available online 11 August 2021

Keywords:
Capacitive stimulation
Bioreactor design
Finite element modelling
Homogeneous electric field
Cell elongation
Nuclei aspect ratio
Cytoskeleton orientation
Stem cell osteogenesis
Titanium implant

ABSTRACT

Electrical stimulation of cells allows exogenous electric signals as stimuli to manipulate cell growth, preferential orientation and bone remodelling. In this study, commercially pure titanium discs were utilised in combination with a custom-built bioreactor to investigate the cellular responses of human mesenchymal stem cells via in-vitro functional assays. Finite element analysis revealed the homogeneous delivery of electric field in the bioreactor chamber with no detection of current density fluctuation in the proposed model. The custom-built bioreactor with capacitive stimulation delivery system features long-term stimulation with homogeneous electric field, biocompatible, sterilisable, scalable design and cost-effective in the manufacturing process. Using a continuous stimulation regime of 100 and 200 mV/mm on cp Ti discs, viability tests revealed up to an approximately 5-fold increase of cell proliferation rate as compared to non-stimulated controls. The human mesenchymal stem cells showed more elongated and differentiated morphology under this regime, with evidence of nuclear elongation and cytoskeletal orientation perpendicular to the direction of electric field. The continuous stimulation did not cause pH fluctuations and hydrogen peroxide production caused by Faradic reactions, signifying the suitability for long-term toxic free stimulation as opposed to the commonly used direct stimulation regime. An approximate of 4-fold increase in alkaline phosphatase production and approximately 9-fold increase of calcium deposition were observed on 200 mV/mm exposed samples relative to non-stimulated controls. It is worth noting that early stem cell differentiation and matrix production were observed under the said electric field even without the presence of chemical inductive growth factors.

Statement of significance

This manuscript presents a study on combining pure titanium (primarily preferred as medical implant materials) and electrical stimulation in a purpose-built bioreactor with capacitive stimulation delivery system. A continuous capacitive stimulation regime on titanium disc has resulted in enhanced stem cell orientation, nuclei elongation, proliferation and differentiation as compared to non-stimulated controls. We believe that this manuscript creates a paradigm for future studies on the evolution of healthcare treatments in the area of targeted therapy on implantable and wearable medical devices through tailored innovative electrical stimulation approach, thereby influencing therapeutic conductive and electroactive biomaterials research prospects and development.

1. Introduction

The global market of dental and orthopaedic implants is now weighted at $5.1 billion and $52.8 billion, respectively, in the year 2017. With a compound annual growth rate (CAGR) of 6.6% and 3.8%, the correspondence forecast of dental and orthopaedic implants are expected to worth $7.5 billion and $66.2 billion in the year 2023 [1,2]. Commercially pure titanium (cp Ti) is amongst the most widely used implant material due to its exceptional biocompatibility, great corrosion resistance, high specific strength to weight ratio (tensile strength of 550 MPa [3] and elastic modulus of 110 GPa [4]), and exceptional osseointegration properties [5–9]. The formation of oxide layer that is readily found on the surface of

☆ Part of the Special Issue on Conductive and Electroactive Biomaterials and Bioelectronics, guest-edited by Professors Jonathan Rivnay and Mehdi Nikkhah.

* Corresponding author.
E-mail address: sarah.cartmell@manchester.ac.uk (S.H. Cartmell).

https://doi.org/10.1016/j.actbio.2021.08.010

titanium protected the titanium from corrosion damage caused by physiological changes or biological variations such as metabolism rate, pH, charges and temperature, making it an exceptional material for medical and biochemical applications [10–13]. In recent years, there has been an increasing interest in surface treatment [14,15], modification [16,17], alloying [18,19], and the application of external stimuli [20,21] to amplify the efficacy of Ti-based implant material.

The rapid advances of electrical stimulation (ES) as an external stimulus have brought an extensive amount of attention in ranges of clinical approaches to improve fracture healing and bone remodelling [22–24]. In particular, ES was affirmatively applied in numerous studies to treat and reduce the risk of bone non-union [25–27]. Dental implants can also benefit from the directionality guidance and improved osseointegration provided by ES [28–30]. It is proven, from previous studies, that electrical stimulation on titanium-based surfaces could increase the their morphology and bioelectrochemistry properties, which in turns enhances the efficacy of titanium implantation and promotes bone healing processes [13,31,32]. Despite the promising effects of both cp Ti and ES on bone-related applications, there are only a limited amount of studies combining these two smart notions into an independent conceptual study. Our research aims to utilise cp Ti as a conductive substrate in an electrical regime with the hypothesis that the integration of cp Ti and ES could synergistically improve stem cell osteogenesis.

In addition to bone tissue engineering, researchers in the last three decades have collectively proven that ES provides potential benefits for wound healing [33–37] and spinal cord rehabilitation [38–43]. The efficacy of ES mainly involves the presence of an electric field (EF), which is capable of inducing biochemical and biophysiological responses [44–47]. Although it has been observed that the strength of EF could influence the biological behaviours, the underlying principle of electrically-induced osteogenesis is not fully understood.

Direct stimulation usually involves ES system with conductive electrodes (made up with low or non-corrosive materials) being positioned in contact with the culture medium [28,48]. This ES regime provides an actual amount of potentials between the anode and cathode. The EF can be estimated using the applied voltage per distance between the two electrodes. In all other ES system, the relative EF and current density (CD) distributions can be modelled using three-dimensional finite element model analysis [33,49,50]. The computer simulation allows one to visualise the outcomes of the ES system even before the construction of the real set of experiment. It empowers one to select the final design setup in alignment with the research objectives.

Compared to direct stimulation, the isolation of electrodes from the medium permits capacitive stimulation to be a better option in terms of the avoidance of unwanted Faradic by-products (such as hydrogen peroxide and free radicals which contribute to pH changes) and low to no fluctuation of CD during the stimulation [51,52]. Although a considerably higher potential is needed to achieve the same EF when using direct stimulation, capacitive stimulation is capable of generating a more homogeneous EF across the system to ensure that equal amount of stimulation signal can be delivered equally to every cell regardless of the position within the ES system [53,54]. It is possible to minimise the production of the reactive Faradic by-products by introducing an agar salt bridge between the cell vessel and external electrodes immersed in a buffered solution [47], but it is reported that the effectiveness of this configuration can be massively restricted as it depends heavily on the adsorption of proteins on the electrodes [55].

Several seminal studies conducted by Ercan et al. [21,56,57] suggested that direct stimulation using a commercially available multi-channel electrical stimulator has increased osteoblast proliferation and decreased *Staphylococcus aureus* biofilm growth on anodised nanotubular cp Ti substrate. The positive effect on osteoblast functions and antibacterial properties upon ES have given a robust fundamental basis to this research, proving the potential adaptation of cp Ti substrate and electrical stimulation. It is notable that the studies proposed by Ercan *et al.* have employed direct stimulation for one hour each day for up to three weeks.

Building on this promising data demonstrated by Ercan *et al.*, we proposed to design a system that used capacitive rather than direct stimulation to reduce or eliminate Faradic by-products. Also, we examined ways to optimise the stimulation regime rather than use an ES regime of one hour per day, which has been frequently used in other studies. In consideration of the prospective clinical and physiological application in an amputated limb, it is a continuous stimulation rather than one hour of stimulation per day during the treatment and recovery; a system with a more homogenous stimulation wherein the cells surrounding the cp Ti disc can be equally stimulated is also more favourable.

In order to address these research questions, we have designed a viable, reusable, sterilisable and cost-effective ES bioreactor setup for use in biological laboratory tests. Using Finite Element Analysis, we have optimised the design of the bioreactor that would deliver homogenous ES regime on cp Ti disc in the culture medium. The cellular responses on the cp Ti disc with the combination of ES were also investigated by analysing the stem cell activity over the period of 14 d under continuous capacitive stimulation.

2. Materials and methods

2.1. Capacitive ES bioreactor design and finite element modelling

A three-dimensional assembly of the capacitive ES bioreactor design was created using SolidWorks CAD package 2017 version (Dassault Systèmes) before exported to COMSOL Multiphysics® v5.2 (COMSOL Inc.), a finite-element simulation software used to perform *in-silico* modelling of the EF and CD distribution within the bioreactor. The bioreactor model was designed in such a way that vertically placed conductive electrodes were embedded and insulated by polymer structures, which in isolation to the culture medium reservoir, as illustrated in Fig. 1c.

As the modelling of the capacitive stimulation models may give rise to the fringing field, the capacitance of the bioreactor system was computed to predict the optimal radius of air sphere domain for the boundary condition used in the modelling (Fig. 1d). The plotted graphs showed that sphere radius between 100 and 180 mm would provide an accurate capacitance evident by the convergence of the numerical data. 120 mm was chosen as the radius of the air domain of the bioreactor, as illustrated in Fig. 1e. The parameters used in the computational modelling were listed in Table 1, 120 mm was chosen as the radius of the air domain. Other settings employed in the COMSOL finite-element simulation includes *Electrostatics* interface which solves Gauss' Law was used to compute the electric field, electric displacement field and potential distribution in dielectrics; *Charge Conservation* was assigned to all domains; *Zero Charge* was assigned to the exterior boundaries

Table 1
The parameters used in the computational modelling.

Materials	Electrical conductivity, σ (S/m)	Relative permittivity, ε_r
Titanium disc (grade 4) [31,58–60]	7.4×10^5	1
Culture medium [61,62]	1.7	80
Tissue culture plastic [63]	n/a	2
Electrode [63]	n/a	1
Air [63,64]	n/a	1

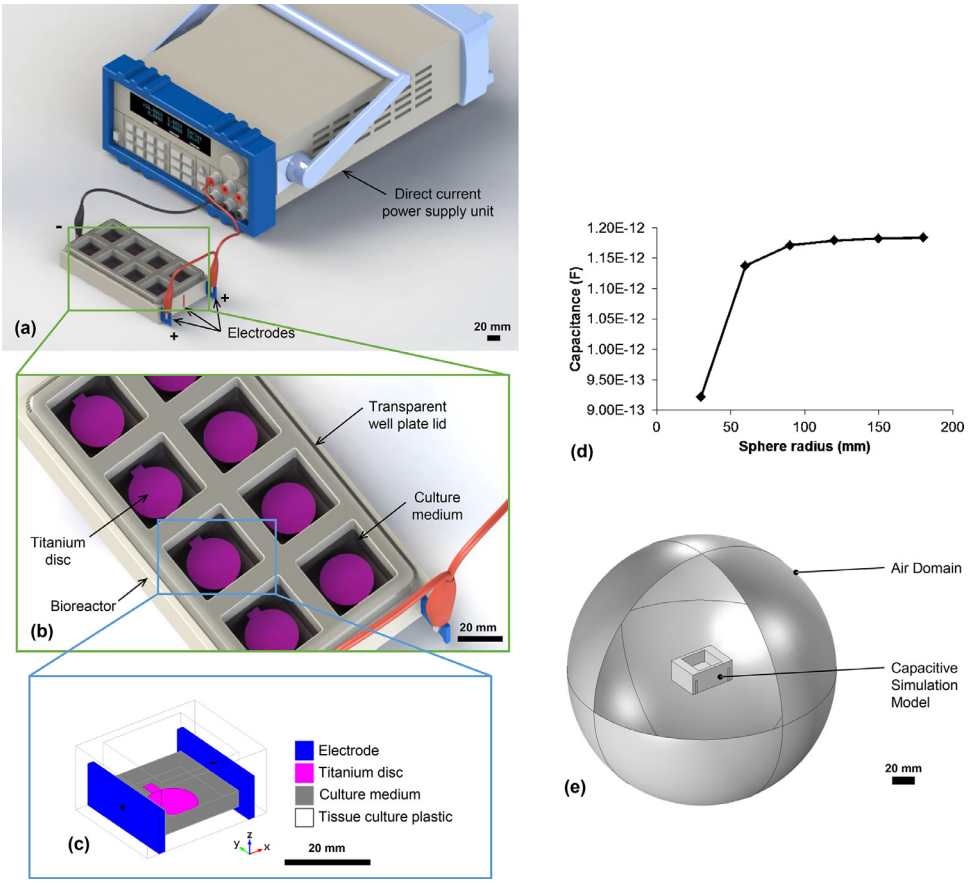

Fig. 1. (a) Full electrical stimulation experimental setup and (b) close view of in-vitro bioreactor assembly; (c) Geometry and components of bioreactor design; (d) Relationship between spherical radius of the air domain and capacitance of the system for capacitive stimulation models; (e) Geometry with air domain for finite element modelling.

of the air volume; *Stationary Study* step was computed, and a 30 V potential difference was assigned between the electrodes to simulate the applied experimental constant potential. Approximately 300,000 tetrahedral mesh elements were generated for the model.

2.2. Cell culture

Human mesenchymal stem cells (hMSCs) from bone marrow were obtained commercially (PT-2501, Lonza Group Ltd., UK). Frozen vials of cells were thawed, cultured and expanded to reach the desired confluency based on the instructions provided by the company. Cells of passage 8 were cultured in growth medium (GM) consisting of Dulbecco's Modified Eagle's Medium (DMEM) with 4500 mg/L glucose, L-glutamine, and sodium bicarbonate, without sodium pyruvate, supplemented with 10% fetal bovine serum (FBS) and 1% Penicillin/Streptomycin (10,000 units/mL) all obtained from Sigma-Aldrich, UK. The cells were maintained at 37°C and 5% CO_2 in a humidified incubator.

The as-received commercially pure Ti discs grade 4 (14 mm diameter, 0.25 mm thick, 99.5% purity, Alfa Aesar, UK) were ultrasonically cleaned and degreased followed by air drying. The surface roughness on the cp Ti disc was around 8–13 nm [65,66]. The cp Ti discs were designed with a tag to assist handling of specimens using tweezers, which could be folded into L-shaped to ease the transference of specimens without damaging the living cell culture during *in-vitro* experiments.

Before cell seeding, a water-repellent circle is drawn on the edge (width approximately 3 mm) of the cp Ti disc (diameter 14 mm) using a PAP pen (Thermo Fisher Scientific, UK), leaving an 8 mm diameter of working area on the cp Ti disc for the cells to be seeded on. The water repellent circle acted as a boundary to limit the cells fluid pooling within the working area of the disc and to ensure that the cells fluid was evenly spread within the capped circle for the cells to adhere securely on the surface of cp Ti disc. Before cell seeding, a water-repellent circle is drawn around the top edge of the cp Ti disc using a PAP pen (Thermo Fisher Scientific, UK) to keep the cell seeding fluid pooled in a single droplet on the surface of cp Ti disc.

All the cp Ti discs were then sterilised using ultraviolet (UV) light for 45 min each side. 100 µL of cell fluid containing 1×10^4 cells were seeded on each of the cp Ti discs. After one hour of cell seeding, GM was added to each well carefully from the wall of the well plate to minimise the turbulence of medium in the well. One day after the initial cell seeding (termed Day 1), half of the samples were refreshed with GM ($n = 8$). The other half ($n = 8$) were treated with osteogenic medium (OM), prepared by adding 50 mg/mL ascorbic acid, 10 mM β-glycerophosphate and 10 nM Dexamethasone (Sigma-Aldrich, UK) to the GM. The non-stimulated control group was incubated in a separate incubator with identical conditions but without electrical stimulation. The media were changed every three days.

2.3. In-vitro *electrical stimulation*

The full *in-vitro* electrical stimulation experimental setup was displayed in Fig. 1a. The ES bioreactor (Fig. 1b) is custom built as a replica of the simulated model, which provides homogeneous EF and no CD, according to the simulation. Briefly, the 8-well polyte-

trafluoroethylene (PTFE, Alfa Aesar, UK) bioreactor consists of three embedded stainless-steel electrodes (Alfa Aesar, UK), i.e. two positive electrodes located on both sides of the bioreactor, one negative electrode located in the middle of the bioreactor to separate the four wells from each side of the bioreactor, creating an inverted symmetry well configuration. The bioreactor was sterilised in a steam autoclave before the *in-vitro* experiments.

On Day 1, the cp Ti discs seeded with cells were transferred to the bioreactor using sterilised tweezers. The bottom of the cp Ti discs was smeared with autoclave sterilised Dow Corning high-vacuum silicone grease (Sigma-Aldrich, UK) to ensure a fixed position of cp Ti discs during the stimulation and expose the cells to constant direction of EF. The smearing procedure was performed by gently pressing the disc bottom onto the grease and removing with a sudden vertical motion for even distribution of grease on the disc bottom, as described by Ryan [67]. The cp Ti discs were then fixed in the middle of the bioreactor with the tag of cp Ti disc faced upwards and paralleled to the electrodes, where the left side of the disc was positioned near to the positive terminal, and right side of the disc was positioned near to the negative terminal, aligned according to the abovementioned inverted symmetry. The tag was present on the cp Ti disc to allow for tracking of sample position and to aid sample handling. GM and OM were added to respective wells of the experimental group and secured with the lid of standard cell culture plates (Sigma-Aldrich, UK).

The bioreactor was connected to a calibrated Triple Output Programmable Direct Current Power Supply (Model 9130; B&K Precision Corporation, Yorba Linda, CA, USA). The full setup of the experiment is displayed in Fig. 1a. Continuous stimulation with constant potentials of 14.2 V and 28.4 V was applied to the bioreactor, corresponding to, respectively, 100 mV/mm and 200 mV/mm simulated EF obtained from the modelling data (Fig. 2c). The experimental group was incubated under standard conditions during the ES. The media were changed every three days. All assays were performed immediately after last exposure to the EF.

Samples were harvested at two time points, Day 7 and Day 14, for AlamarBlue™ assay ($n = 8$); viability and morphology assessment using LIVE/DEAD cell viability assay ($n = 4$); and Day 14 for cell lysate collection for alkaline phosphatase (ALP) ($n = 8$); calcium concentration using alizarin red staining quantification assay ($n = 8$); and nuclei aspect ratio and cytoskeleton orientation measurement using immunofluorescence staining assay ($n = 4$).

2.4. AlamarBlue™ assay

To assess the cellular metabolic activity, the control and stimulation groups were assayed at day 7 and 14 using AlamarBlue™ assay. Briefly, 300 µL AlamarBlue™ mixture containing 10% AlamarBlue™ stock solution (Thermo Fisher Scientific, UK) and 90% cell culture medium (GM) was added directly to the samples in a 24 well plate, then incubated at 37°C for 60 min. Following incubation, three 50 µL replicates of the aliquots were transferred from each sample into a clear 96 well plate. Fluorescence readings were taken using a FLUOstar OPTIMA microplate reader (BMG Labtech) at 560 nm excitation, 590 nm emission. After the assay, the samples were washed with fresh GM and replaced with respective media (GM or OM). The same samples were measured at each time point.

2.5. LIVE/DEAD cell viability assay

Cell viability and morphology on the cp Ti disc upon ES was assessed by a fluorescence-based LIVE/DEAD cell viability assay (Thermo Fisher Scientific, UK). The assay was performed at day 7 and 14. 4 mM calcein-AM in anhydrous dimethyl sulfoxide (DMSO)

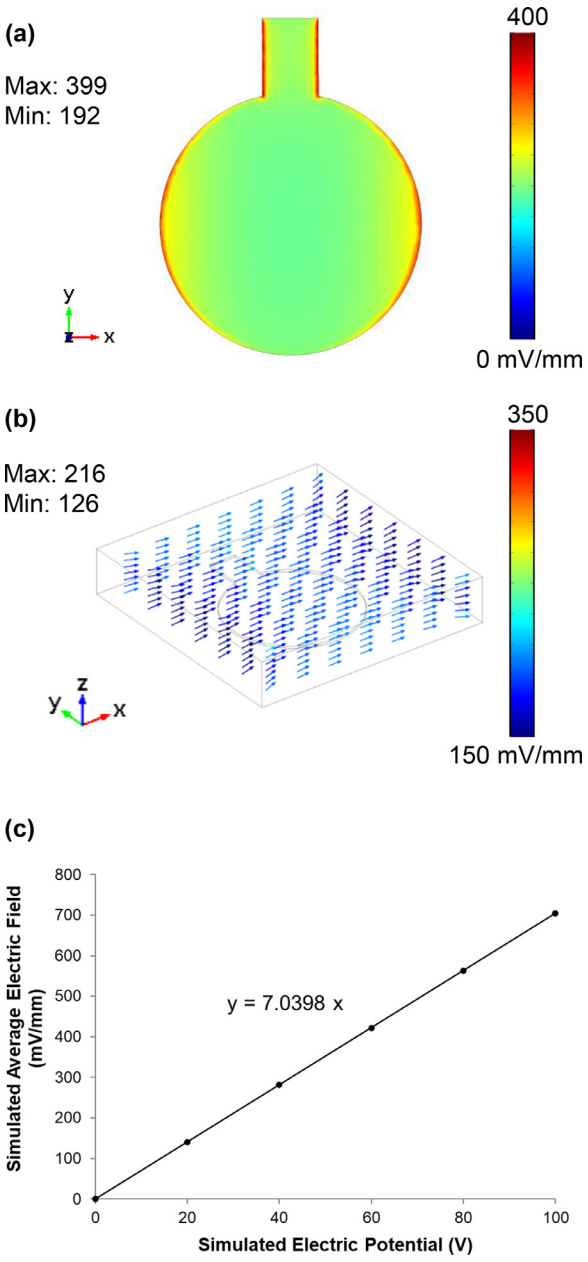

Fig. 2. Electric field distribution (mV/mm) on (a) the titanium disc and in (b) the culture medium. The maximum and minimum electrical field values are shown at the top-left corner. Note that there was no simulated current density. (c) Relationship between simulated average electric field and simulated electric potential on the titanium disc.

and 2 mM ethidium homodimer-1 in DMSO/H_2O 1:4 (v/v) in phosphate buffered saline (PBS) were added to each sample and incubated for 30 min, washed again with fresh PBS, and visualised using a fluorescence light microscopy (Nikon Eclipse 50i, equipped with Lucia GF-DXM1200 version 4.82 imaging software).

2.6. Cell lysate preparation

Cell lysis was performed to allow the extraction of intracellular contents such as proteins, lipids, and nucleic acid. At day 14, the samples in a 24 well plate were washed twice with PBS before a 300 µL of Gibco® EDTA-free 0.25% Trypsin solution (Thermo Fisher Scientific, UK) was added to each sample and incubated for 4 min. Mild vortex and gentle tapping were performed following incubation to ensure that the cells were detached from the samples. The

trypsinised cells were transferred to a 1.5 mL microcentrifuge tube. 300 µL of GM was added twice to the well plate to wash and collect the leftover cells, then transferred to the same microcentrifuge tube and centrifuged at 300 g for 5 min. Following centrifuge, the supernatant was removed, and 250 µL of ALP assay buffer (BioVision, UK) was added to the cell pellet with an addition of the high-speed vortex to lyse the cells. The cell lysate was kept at -70°C for further use.

2.7. Alkaline phosphatase (ALP) assay

The level of alkaline phosphatase (ALP) activity indicates an early marker of osteogenic differentiation. Before performing the ALP assay, the cell lysate was centrifuged at 13,000 g for 3 min to remove insoluble material. The ALP colourimetric assay kit (BioVision, UK) was used to measure the ALP activity in the samples. The *p*-nitrophenyl phosphate (*p*NPP) working solution was prepared according to the manufacturer's instruction. ALP assay buffer and stop solution were readily prepared in the assay kit. To begin the assay, an optimal volume of cell lysate was aliquoted to a clear 96 well plate in duplicate, and the ALP assay buffer was added to bring the total volume to 80 µL. 20 µL of stop solution was added to one of the duplicated lysate mixtures (as background reading) to terminate the ALP activity. 50 µL of 5 mM *p*NPP solution was added to all the mixtures and incubated for 60 min at room temperature protected from light. The reaction was stopped by adding 20 µL of stop solution to the reacted samples (as sample reading), making a total volume of 150 µL in each well. The absorbance readings were taken using a Multiskan Ascent Microplate Reader (LabSystems, Inc.) at 405 nm. The actual absorbance reading of the sample was obtained by subtracting the background readings from the sample readings.

2.8. Alizarin red staining quantification assay

The level of bone mineralisation and calcium deposition in the cell culture were determined by alizarin red staining. At day 14, the control and experimental groups were washed twice with PBS and fixed with 10% formalin solution (Sigma-Aldrich, UK) for 15 min at room temperature. The fixed cells were then washed three times with deionised (DI) water. The samples in the 24 well plate was stained 30 min with 2% w/v alizarin red staining solution (Sigma-Aldrich, UK) in DI water and maintained at pH 4.1–4.3. The staining solution was removed, and the samples were washed five times with DI water. For quantitative analysis, the red-stained calcium contents were dissolved at 37°C for 30 min with gentle shaking using 300 µL of 10% w/v cetylpyridinium chloride (CPC) (Sigma-Aldrich, UK) in PBS. Subsequently, three 50 µL replicates of the dissolved solution were pipetted from each sample into a clear 96 well plate. Absorbance readings were taken using a Synergy II plate reader (Biotek Instruments Ltd.) at 550 nm.

2.9. Immunofluorescence staining

After cells were fixed using 10% formalin solution (Sigma-Aldrich, UK) for 15 min at room temperature, they were washed three times with PBS and permeabilised with 0.1% Triton X-100 in PBS for 10 min at room temperature. The cell cytoskeleton filaments (F-actin) were stained with Alexa Fluor® 488 phalloidin (1:1000 dilution, Invitrogen) for 30 min and carefully mounted with ProLong® Gold Antifade Mountant with DAPI (Thermo Fisher Scientific, UK) to stain the cell nucleus. The samples mounted on glass slides and coverslips were sealed with transparent nail polish for microscopy imaging using a fluorescence light microscopy (Nikon Eclipse 50i, equipped with Lucia GF-DXM1200 version 4.82 imaging software). Images captured were then used to quantify the nuclei aspect ratio ($n = 25$) and cytoskeleton orientation ($n = 600$). The length and angle were manually traced using ImageJ software. The nuclei aspect ratio was determined by the ratio of the longest to the shortest dimension of the stained nuclei (blue), where 1.0 was considered fully rounded nucleus and 0.1 was considered a high extent of elongation. The angle of cytoskeleton orientation was measured as the angle between the cell major axis and the direction of the electric field, i.e. positive (+) terminal as 0° and negative (-) terminal as 180°.

2.10. H_2O_2 concentration and pH measurements

H_2O_2 concentration in the media was detected using a fluorimetric hydrogen peroxide assay kit (Sigma-Aldrich, UK). 50 µL of master mix solution was prepared according to manufacturer's instruction and added to 50 µL of media in a 96 well plate. Room temperature incubation for 15 min and the fluorescence readings were taken using a Synergy II plate reader (Biotek Instruments Ltd.) at 540 nm excitation, 590 nm emission.

The media in cultured were collected during media change and tested immediately with a Checker pH tester (Hannah Instruments, Accuracy: ± 0.2 pH).

2.11. Statistical analysis

Statistical significance was analysed using the two-tailed paired Student's *t*-test in Microsoft Excel [68]. Data are presented as mean ± standard deviation (S.D.). Probability (*p*-value) less than 0.05 was considered to be significant.

3. Results and discussion

3.1. Capacitive ES bioreactor design and finite-element modelling

As early as the 1960s, the concept of exogenous capacitive stimulation has been employed by Goldenthal as a technique for bilateral and unilateral activation of the diaphragm [69]. Brighton et al. later showed that capacitive stimulation electric field could enhance the *in-vivo* growth plate in a highly consistent manner [70]. Thereafter, the development of capacitive stimulation has been increased gradually following a number of successful *in-vivo* studies that confirmed the efficacy of this non-invasive, infection-free stimulation on bone healing [51,71], spinal fusion [72] and fracture non-union treatments [73,74]. Capacitive stimulation is known to improve the success rate of metallic fixated implantation by promoting bony ingrowth and overcoming the biochemical effects of stress shielding [72]. Furthermore, *in-vitro* studies revealed that the intracellular signalling mechanisms for which the capacitive stimulation modulates the bone remodelling process is different from direct and inductive stimulation, including the regulation of cytosolic calcium through voltage-gated calcium channels [44,51]. However, appropriate strength and homogeneity of the applied electrical signal are desired to attain effective signal transduction in the stimulated cells [74,75].

In this study, cp Ti disc was utilised in combination with a custom-built capacitive ES bioreactor to investigate the cellular responses of human mesenchymal stem cells via *in-vitro* functional assays. We compared four bioreactor designs through the use of finite element simulation to obtain a design that delivers the most homogeneous electric field across the disc. Delivering a homogeneous electric field is a critical factor in designing a bioreactor model. It does not only facilitate the ease of use for anyone who handles the bioreactor, more importantly, but it also ensures that at any position in a single well of the bioreactor receives an equal amount of electric stimuli, including the substrates and cells

that are in the culture. ES on basic cell culture is a two-way process: while the applied EF can induce a change on the cellular transmembrane potentials, the EF can also be perturbed and redistributed by the cells at the same time [76]. However, when a substrate or scaffold is introduced into the ES system, a few other factors should be considered. For instance, the distribution of EF between the substrate and ES system, the change of transmembrane potentials triggered by the stimulated substrate with pre-existing concerns on conductivity, chemical, mechanical and surface characteristics. For this reason, we utilised the pre-tested and biocompatible cp Ti discs in this study, which were trimmed from commercially pure titanium film without additional modification of the surface and chemical composition. Given these facts, by making sure that the electric field is distributed homogeneously across the system would assist us to eliminate the uncertainties contributed by this multifactorial paradigm and to focus only on the interaction mechanism between the cells and the applied EF.

The EF distributions on the cp Ti disc surface and inside the culture medium are plotted in Fig. 2a and b, respectively. In addition to a homogeneous EF distribution both on the cp Ti disc as well as in the culture medium, the design modelled in finite element analysis featured no current density in the medium of capacitive stimulation. This is mainly due to no direct contact of the electrode in the ionic medium during the stimulation, and the electrostatic EF is delivered indirectly through the capacitance of the electrodes external to the culture medium. The isolation of the stainless-steel electrodes which are embedded in the PTFE chamber ensures that no direct contact of the metallic electrode in any near to the culture medium (Fig. 1c). With this non-invasive approach, the concerns of electrochemically induced pH changes and radical species can be minimised or even eliminated [77]. At the same time, all the components contained in the chamber will have an equivalent stimulation regardless of the position in the chamber [24]. This gives an added benefit to an ES system because the possible occurrence of imbalanced or partial stimulation will be disregarded, in addition to no simulated CD is computed with this model. In spite of that, a relatively higher potential is required to maintain the desired EF, as compared with other models, because the EF is partially impeded by the PTFE layer that separates the culture medium and the electrode. This simulated bioreactor model displayed a significantly uniform and small difference as compared to conventional direct stimulation, i.e. 2-fold difference, in the EF strength across the cp Ti disc. In the culture medium, higher EF strength was discovered in the culture medium near to both of the electrodes, where almost linear vector distribution was observed. To understand the relationship between the EF magnitude and applied voltage of the model, the average simulated EF magnitude on the cp Ti disc with varying simulated input voltage was computed and plotted (Fig. 2c). When setting up the stimulation experiment using our custom-built capacitive ES bioreactor design, the actual direct current voltage reflected to stimulate desired EF can be estimated by the projected graph based on the linear equation of $y = 7.0398^{*}x$, where y is the average simulated EF and x is the simulated voltage. In a physiological manner, direct contact with high voltage might impose a risk to the user of the device. However, a capacitive simulation electrotherapy device is non-percutaneous and can be regarded as a wearable device because the signal generator is typically encapsulated in an insulated case made from resistive materials that are capable of promoting continuous, perpetual stimulation for rapid healing [78–80].

3.2. In-vitro *capacitive electrical stimulation*

Preliminary studies were conducted to deduce the optimal ES regime for use in the *in-vitro* experiments. 10 and 50 mV/mm simulated EF was initially tested using the bioreactor, but there was a minimal effect on the hMSCs. Hence a higher EF was chosen for the present work. As 30 V (i.e. 211 mV/mm) was the maximum allowable potential difference that can be generated using the direct current power supply unit, we presented data from 100 and 200 mV/mm simulated EF in this work.

The custom-built ES bioreactor (Fig. 1b) featured some prominent attributes for *in-vitro* assessments. The bioreactor made from PTFE main chamber and embedded stainless steel electrode can be manufactured in a reasonable cost (under £30 per set, price as of the year 2020), can be sterilised under high heat humidified autoclave, can stimulate a sample size of 8 in one batch, and have the potential to scale up the production and sample size. The position of cp Ti disc partially fixed using medical grade silicone grease in the culture would also give the advantage to visualise the effect of ES on preferential alignment of the cells cultured on the cp Ti disc. The power supply of our setup brought about a limitation to our study, although this did not impact the main aim. As the allowable voltage range of the direct current power supply was between 0 and 30 V, and 30 V was reflected as 211.2 mV/mm simulated EF, according to the linear equation computed in the simulation. Given this point, any EF desired above the aforementioned EF was not achievable due to the limit of the power supply. However, in future work, a power generator with a wider voltage range can be incorporated in the experiment, to have a broader understanding on influence of the high EF strength on cellular responses, and to appreciate the upper EF threshold that the cells can hold up to, ultimately maximising the regulation of ES in *in-vitro* investigations, as alleged in one of the previous studies [81].

For the selection of EF wise, Qi *et al.* previously compared different ES intensities delivered via a direct stimulation on olfactory unsheathing cells through a biodegradable conductive composite made of conductive polypyrrole (2.5%) and biodegradable chitosan (97.5%), had concluded that 100 mV/mm were able to promote proliferation and differentiation expressions, but ES intensity above 300 mV/mm could induce apoptosis, and 1000 mV/mm would lead to a destruction of healthy cells [82]. On another study, Banks *et al.* reported cell viability was maintained on EF strengths between 20 mV/mm to 200 mV/mm showed high cell viability, but 300 mV/mm evinced a slightly lower viability but retained a maximum migration ability, while cell death was discovered on EF strength of 500 mV/mm within 5 h of ES application [47]. Studies conducted by Mooney *et al.* and Canillas *et al.* confirmed that 150 mV/mm would sustain cell proliferation and cytoskeletal orientation with the ability to differentiate into specific functional cells [83,84]. Furthermore, Bai *et al.* and Petrov *et al.* have elucidated that 200 mV/mm and 250 mV/mm, respectively, did not inhibit the upregulation of long-term growth factors and preferential alignment of cell network [85,86]. All things considered, we believe that our selected EF range, i.e. 100 mV/mm and 200 mV/mm simulated EF would give an adequate understanding on how ES affects the cellular mechanism, although a higher EF is limited by the power supply.

The bioreactor setup in the present study effectuated a continuous stimulation without compromising cell viability. The *in-vitro* viability assays revealed a denser cell number at an increasing EF intensity. It is important to stress that a continuous stimulation is of prominence in some practical electrophysiological applications. A perpetual flow of electrical signal at an appropriate regime does not only facilitate rapid healing in a fraction of time, but it would also reduce the treatment cost in a long run because there is no need for the patient to attend to the rehabilitation centre periodically to receive electrotherapy from the practitioners. In some previous works, a long-term stimulation was not achievable. Especially for those using direct stimulation methods, Hu et al. demonstrated that direct stimulation on polypyrrole (PPy) conductive films with a magnitude of 35 mV/mm evinced the best cell viability and

calcium deposition rate exhibited on stimulation time of 4 h per day; while 12 h of stimulation would dramatically reduce the cell activity and cause cell death [87]. Liu *et al.* further established in their study that direct stimulation of 15 mV/mm for above 6 h per day would cause a reduction in cell proliferation and differentiation abilities, while 1 h stimulation per day would lead to increased viability and earlier differentiation relative to 0.5 h per day because it was believed that the induction of osteogenesis is strongly related to the time-dependent intracellular calcium ion signalling pathway, where 1 h per day of stimulation was sufficient to induce a transient change in intracellular Ca^{2+} concentrations [88]. On the contrary, Kim et al. suggested that a direct stimulation with biphasic electric current would promote cell survival upon continuous stimulation (24 h per day) for 4 d, and increase the production of vascular endothelial growth factor (VEGF), an essential mediator for bone repair and regeneration, but did not induce cell differentiation [89]. Using salt-bridge configuration, Bai *et al.* confirmed that EF of 200 mV/mm for 24 h of stimulation have no significant difference in the upregulation rate of VEGF with 4 and 8 h of stimulation, indicating a better ES system for use in comparison with direct stimulation [85].

Fitzsimmons et al. suggested that a continuous stimulation was made possible with the use of capacitive stimulation, where an approximate of 3-fold increase of tibial collagen production was attained in comparison with non-stimulated controls, although an EF exposure of 30 min per day was able to improve bone matrix formation when compared with non-stimulated controls [90]. A further investigation conducted by Hartig *et al.* confirmed the positive effect of long-term *in-vitro* capacitive stimulation in inducing bone matrix maturation with the significant synthesis of fibronectin, type-I collagen, proteoglycans, osteocalcin and other osteogenic expressions upon a course of 18-day continuous stimulation as compared with non-stimulated controls [91]. On another study, Brighton *et al.* compared three different types of ES delivery systems on MC3T3-E1 mouse osteoblastic cells, namely capacitive, inductive and combined electromagnetic fields [44]. They concluded that 24 h of capacitive stimulation (2 mV/mm) resulted in the best proliferation among all delivery systems; although a significant proliferation relative to non-stimulated controls also observed on two other delivery systems, the rate of proliferation was stagnant after the first 30 min of stimulation. However, the capacitive stimulation did not increase the intracellular Ca^{2+} release as compared to both the inductive and combined electromagnetic field. It was explained that the signal transduction pathways of capacitive stimulation is not a straightforward process, where the mechanism of cytosolic Ca^{2+} secretion via capacitive stimulation is translocated through the voltage-gated calcium channels of the plasma membrane which then increases the intracellular calcium concentration, whereas the signalling of cytosolic Ca^{2+} release corresponding to inductive and electromagnetic field was directly transduced by intracellular calcium storage [51].

3.3. Cell viability, morphology and preferential alignment

Titanium has been recognised as a promising bone implant material thanks to its exceptional corrosion resistance, biocompatibility and high specific strength. Commercially pure titanium is amongst the most widely used Ti-based materials nowadays, especially in dental and bone replacement procedures [5,92]. In the present study, cp Ti discs without ES (at 0 mV/mm) have attained good MSCs viability, proliferation, osteogenic differentiation and bone cell mineralisation. The cells cultured in both growth and osteogenic medium evinced a doubling of metabolic activity from day 7 to day 14 in culture. The growth medium exhibited a higher metabolism rate than the osteogenic medium in general, which has been considered a typical phenomenon [93]. This is because osteogenic medium comprised of growth factor to induce specific functionalised differentiation of stem cells over time, while the growth medium maintained the normal growth and multiplication of cells without chemically inducing the specific differentiation [94]. The more apparent effect of osteogenic induction can be observed in differentiation assays.

AlamarBlue™ assay evinced that a significant increase in cellular metabolism rate was observed on 200 mV/mm as compared to that of control (non-stimulated) and 100 mV/mm (Fig. 3a). For growth medium (GM), a significant increase of cell metabolic activity is seen as the EF increased to 100 mV/mm and 200 mV/mm for both day 7 and day 14. For osteogenic medium (OM), an increasing trend was also displayed as the EF increases. As compared to the control group (OM day 14), it is demonstrated that an approximately 5-fold increase of cell metabolism rate on 200 mV/mm on OM day 14. OM day 7 on 100 mV/mm, however, showed a higher proliferation rate as compared with OM day 7 on 200 mV/mm.

The metabolism rate has displayed an increasing trend at an elevated EF intensity (Fig. 3a). It is worth noting that the growth medium, on both day 7 and 14, has a linear escalation with the increase in EF intensity, but osteogenic medium on 100 mV/mm has shown a higher metabolism rate than 200 mV/mm on day 7 followed by a plateau. This finding was not reported in any other capacitive stimulation regime, but it might be related to a combinational effect of the modulation of electrochemically active molecules at this particular EF intensity [95,96] correlating with the polarisation of intracellular potential which triggers the cytoskeleton activation in directing cell migration and orientation [97]. This combination effect was not observed in 200 mV/mm because the dominating potential difference in conjugation with the higher EF has overcame the polarisation at an earlier stage of cell development and activated early cell migration [98,99], which also explain the most oriented cell alignment under EF exposure of 200 mV/mm, even on day 7 in culture (Fig. 4c and e). Some studies demonstrated that the cell proliferation rate in capacitive stimulation delivery system is mediated by cytoskeletal calmodulin pathway which is activated by intracellular calcium concentration via transmembrane voltage-gated calcium channels [44,52].

None of the cells exposed to 100 and 200 mV/mm showed signs of toxicity. As the cp Ti discs were fixed in position, the cells on the cp Ti discs could experience a constant vector of EF at any time point during the experiment. In comparison to non-stimulated controls, the Live/Dead Imaging (Fig. 4a–j) showed that hMSCs cultured on the discs were majority aligned in a direction and greatly stretched across the discs – either multiplying themselves or differentiating into osteoblastic cells. The cell morphology exhibited in LIVE/DEAD assay demonstrated that the cells on cp Ti disc aligned perpendicularly to the direction of EF. While, in general trend, both GM and OM have better cell growth and coverage on day 14, the increase in EF also promoted higher cell elongation and alignment.

For GM day 7, cells started to demonstrate signs of extension and orientation as the EF increased although the morphological changes were not very significant. For GM day 14, 200 mV/mm (Fig. 4h) showed a significant extension of cells that have an elevated coverage as compared to 100 mV/mm (Fig. 4g). Signs of alignment also became apparent when the EF increased from 100 mV/mm to 200 mV/mm.

Due to the osteogenic conditions provided to cells, the hMSCs cultured in OM exhibited signs of differentiation to osteoblastic cells. A relatively lower sign of differentiation was displayed on OM day 7 on 100 mV/mm (Fig. 4d). However, as the EF increased to 200 mV/mm (Fig. 4e), the cells showed a stronger indication of differentiation as the hMSCs proliferated into pre-osteoblastic like cells. Similar to GM day 14, OM day 14 also displayed a greater extent of cell alignment. OM day 14 on 200 mV/mm (Fig. 4j)

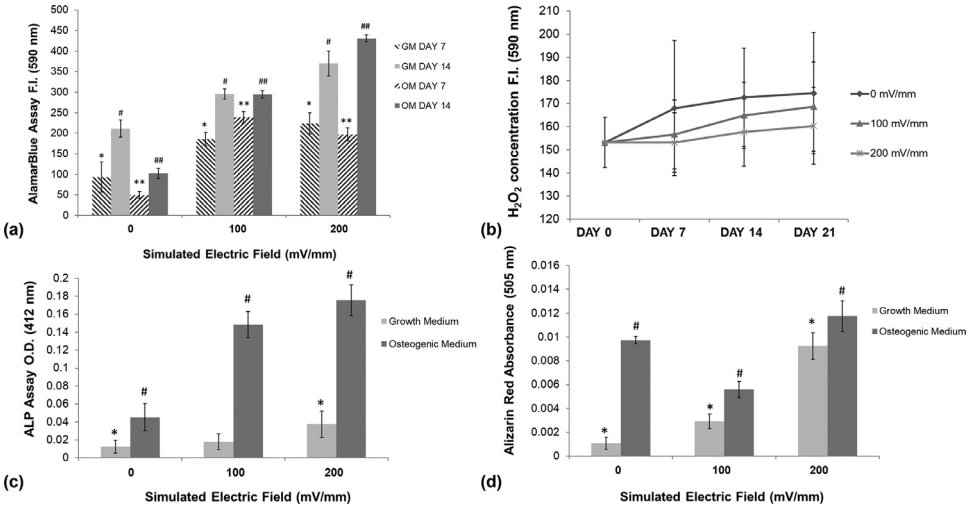

Fig. 3. (a) AlamarBlue™ metabolic activity of hMSCs between control, simulated electric field of 100 mV/mm and 200 mV/mm at Day 7 and 14 in growth medium (GM) and osteogenic medium (OM). Values are mean ± S.D., $n = 4$, $^{*}p < 0.05$ compared to GM DAY 7 of 0 mV/mm and respective EF; $^{\#}p < 0.05$ compared to GM DAY 14 of 0 mV/mm and respective EF; $^{**}p < 0.05$ compared to OM DAY 7 of 0 mV/mm and respective EF; and $^{\#\#}p < 0.05$ compared to OM DAY 14 of 0 mV/mm and respective EF. (b) Hydrogen peroxide (H_2O_2) measurements at day 0, 3, 5 and 7 between control, simulated electric field of 100 mV/mm and 200 mV/mm in growth medium. Values are mean ± S.D., $n = 4$, data not statistically significant. (c) Alkaline phosphatase (ALP) activity of hMSCs between control, simulated electric field of 100 mV/mm and 200 mV/mm at Day 14 in growth and osteogenic medium. Values are mean ± S.D., $n = 4$, $^{*}p < 0.05$ compared to Growth Medium of 0 mV/mm and $^{\#}p < 0.05$ compared to Osteogenic Medium of 0 mV/mm. (d) Alizarin red staining calcium concentration quantification assay of hMSCs between control, simulated electric field of 100 mV/mm and 200 mV/mm at Day 14 in growth and osteogenic medium. Values are mean ± S.D., $n = 4$, $^{*}p < 0.05$ compared to Growth Medium of 0 mV/mm and $^{\#}p < 0.05$ compared to Osteogenic Medium of 0 mV/mm and respective Growth Medium.

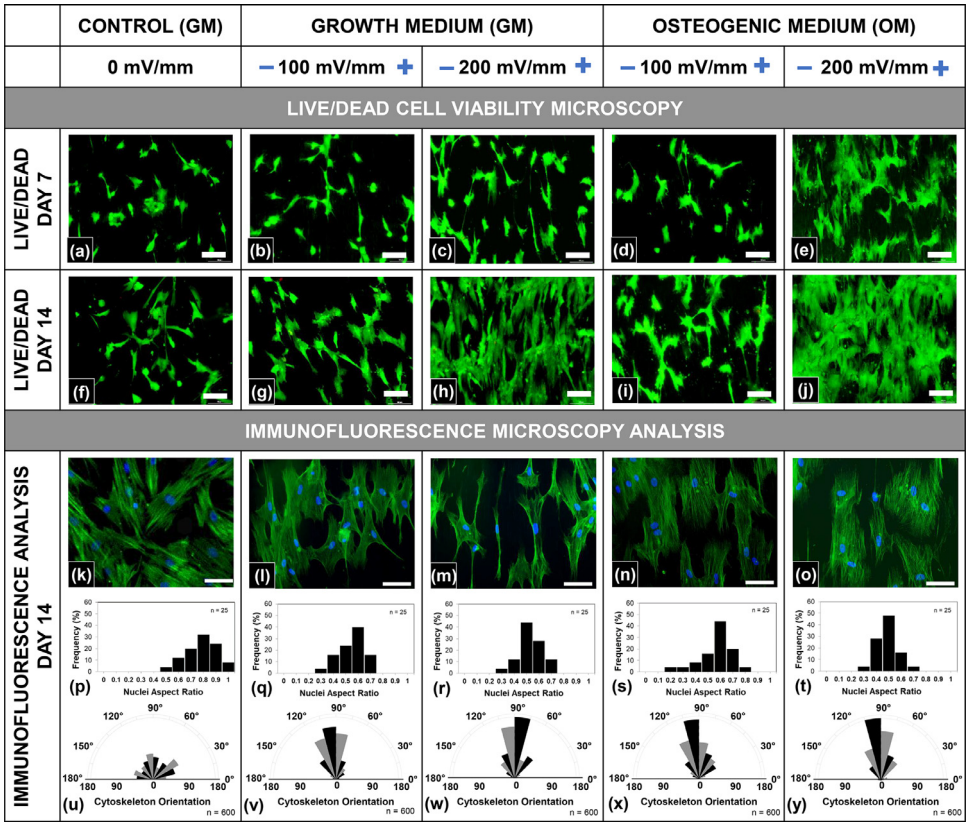

Fig. 4. (a) – (j) LIVE/DEAD cell viability microscopy on titanium disc at Day 7 and 14 in growth and osteogenic medium. Live cells were stained with green and dead cells were stained with red. Scale bar = 100 µm. (k) – (o) immunofluorescence microscopy of cell nuclei (blue) and F-actin cytoskeleton (green) of hMSCs in control (growth medium), simulated electric field of 100 mV/mm and 200 mV/mm at Day 14 in growth and osteogenic medium. Tabulation of nuclei aspect ratio (p) – (t) and rose plot of cytoskeleton orientation (u) – (y) in respective conditions. Scale bar = 100 µm.

demonstrated a significant cell extension and coverage, the differentiated cells have not only shown directionality but also cell matrix maturation.

The immunofluorescence staining of hMSCs on cp Ti disc revealed the ellipticity of cell nuclei (blue) and directionality of the actin filaments (green), as shown in Fig. 4k–o. For comparison purpose, the control group was conducted against the GM on day 14 of culture, while the experimental group was conducted on both GM and OM on 100 mV/mm and 200 mV/mm upon 14 d of continuous exposure to EF. The experimental group demonstrated a highly aligned cell structure with elongated cytoskeleton across the samples as compared with the control group.

Cell morphology and elongation play a critical role in regulating stem cell commitment, especially for the osteogenic differentiation of MSCs [100]. Electrical stimuli are known to promote cell elongation and extension by altering the local electrical fields of extracellular matrix molecules [101], protein adsorption and cell surface receptors to push the cellular membrane in the direction of movement [102]. Cell elongation is mediated by the cytoplasmic actin filaments which support the cytoskeletal membrane structure and transmit intracellular forces to the nucleus [103], leading to the direct correlation between the cells and nuclei aspect ratio [104]. In the present study, the measurements of nuclei aspect ratio (Fig. 4p–t) displayed that the nuclei in the experimental group was more elongated as compared with the control group. The nuclei of the control group exhibited a rather spherical shape with the highest count on the aspect ratio of 0.8; both GM and OM on EF of 100 mV/mm displayed an aspect ratio of 0.6 and 200 mV/mm showed an aspect ratio of 0.5 at the highest counts. The lower the aspect ratio, the more elongated the nucleus is. It is notable that cells stimulated at 100 mV/mm demonstrated a mean nuclear aspect ratio of 0.6 for both GM and OM. Similarly, cells stimulated at 200 mV/mm exhibited a mean nuclear aspect ratio of 0.5 in both media, suggesting that the nuclei were more elongated along the longer axis of their cell body at a higher EF. The findings reflected that the capacitive stimulation was able to enhance a considerable cell stretching in comparison to non-stimulated controls, while EF at a higher intensity could further promote cell elongation. These findings further support the preferred aspect ratio committed by MSCs to differentiate towards osteogenic lineage [105].

It is well known that directional migration and cell network extension can be predominated by the introduction of electric cues. Bone repair and wound healing are some of the examples that explain the mobility of cells through endogenous membrane potentials [106,107]. It is evinced that the actin filaments of cells response positively toward electrical regime and could contribute to the change of cytoskeleton shape and orientation when exposed to EF. For the first time, the effect of capacitive stimulation on MSCs alignment and morphological changes on cp Ti disc is analysed. About 600 actin filaments from images of different regions were measured for the tabulation of data in the rose plot. The control group has an equal dispersion of cytoskeleton orientation from 0° to 180°; cytoskeletons in the experimental groups were more perpendicularly aligned as compared with the control group, i.e. higher counts between 75° and 105° for both media conditions and both EF strengths. The respective calculated percentage of actin filaments that aligned perpendicularly to the direction of EF (75° to 105°) was at 20.5% (control; Fig. 4u), 42.5% (GM 100 mV/mm; Fig. 4v), 53.3% (GM 200 mV/mm; Fig. 4w), 41.3% (OM 100 mV/mm; Fig. 4x), and 46.2% (OM 200 mV/mm; Fig. 4y).

Through the cytoskeleton orientation analysis, it can be seen that the cells were aligned perpendicularly with elongated morphology on the increasing EF intensity. It is encouraging to compare these findings with those found by other researchers, who suggested that the stimulated cells elongated perpendicularly to the direction of field while the non-stimulated controls retained a random orientation [47,83,85,108–112]. This observation may be explained by the fact that the cells elongated and aligned perpendicularly to the direction of applied electric field to minimise the voltage drop across the cells [113–115]. As the EF increases, the cells aligned more vertically as evinced from the increase in percentage from 20.5% (GM control) to 42.5% (GM 100 mV/mm) to 53.3% (GM 200 mV/mm) to minimise the EF gradient across themselves [30].

The structural reorganisation and cell orientation are strongly correlated with the intracellular signalling pathways that lead to functional differentiation [116,117]. Under the influence of ES, the intracellular calcium distribution, a mediator for signal transduction, will accelerate the internal rearrangement of cytoskeletal network and regulate the release of calcium to facilitate bone mineralisation process [118]. On a related note, Mendoza suggested a paradigm to explain the perpendicular alignment of the cells through an adaptation process of retraction and elongation [109]. The adaption process that involved the exertion of tensional force on the cell membrane, initiated by the EF at the anodic and cathodic poles, which later on cause an increase in calcium ions in the cell cytoplasm, followed by a cytoskeletal reorganisation in association to a retraction on the cell body an each side of the electrodes, and subsequently a directional re-extension of lamellae cause an elongation of the cells in perpendicular to the EF. Zhao *et al.* and Kotwal *et al.* further elucidated in their study that the types of culture medium were not a dominating factor contributing to the directionality of the cell alignment, but will facilitate the intracellular growth and reorganisation of cytoskeleton [101,111].

3.4. Stem cell osteogenic response and calcium deposition

Electrical signals have been recognised as a prominent external cue for stem cell differentiation [24]. Several functional assays can be employed to determine the level of stem cell differentiation. Alkaline phosphatase (ALP) activity is a quantifiable marker for osteogenic differentiation of MSCs, and is often used in conjunction with Alizarin Red calcium concentration analysis to measure the bone mineralisation ability of MSCs in culture [119,120]. In the present study, OM in the control group showed a higher ALP activity than GM, denoting a positive promotion of ALP level under osteogenic medium. The combination of osteogenic inducing media and EF revealed a significant enhancement of ALP level of cells cultured on cp Ti disc. ALP activity was highest at OM 200 mV/mm followed by OM 100 mV/mm and OM non-stimulated controls. Compared to the control group, the cells simulated under EF of 200 mV/mm revealed a significant increase (approximately 4-fold) of ALP activity both GM and OM, denoting that EF of 200 mV/mm was capable of inducing osteogenic differentiation even without the addition of osteogenic growth factors.

The cells cultured for 14 d on cp Ti disc showed a significantly higher mineralisation rate on both GM and OM when exposed to EF of 200 mV/mm (Fig. 3d). On increasing EF, a steady increase of calcium content was discovered on GM without the addition of osteogenic growth factors. As compared to the control group, approximately 3-fold and 9-fold increase of calcium contents were evinced on 100 mV/mm and 200 mV/mm, respectively. For OM, there was a significant decline of mineralised calcium on 100 mV/mm than the control group and 200 mV/mm. In general trend, the OM still possessed a higher calcium deposition than the GM. The most striking result to emerge from the findings is that GM 200 mV/mm have a considerable close resemblance to OM non-stimulated controls in both differentiation tests, further signifies that the presence of higher intensity EF could bring about stem cell mineralisation even without the need of chemically induced growth factors.

The major difference between ALP and Alizarin Red detection is that ALP enzyme expression is a predictor of extracellular inorganic phosphate, which acts as a mineralisation promoter [121], while alizarin red is a measurement of the content of mineralised calcium compound, known as calcium pyrophosphate dehydrate (CPPD) crystals [122]. Both methods are extensively used and highly recognised as the prime indicator for osteogenic differentiation. However, as the production of the mineralised matrix occurs at the end point of osteoblast maturation [123], the induction of calcium deposition might not have a confirmatory effect at early time points. Our unanticipated finding is broadly consistent with earlier investigation using ES regime on conductive substrates, where a predominant enhancement of calcium deposition would be more substantial at a later time point, i.e. a minimum of 21 d in culture [124–126]. Other researchers explained this situation as a delayed differentiation because the cells under a specific EF would maintain the proliferative process with unchanged or decreased calcium deposition, and this phenomenon is not uncommon when capacitive stimulation is used in conjugation with osteogenic medium [75,89,91]. The delayed differentiation coupling with increased proliferation often upregulates insulin and fibroblastic growth factors which do not modulate calcium deposition but have shown to enhance bone formation during *in-vivo* implantation [127,128].

There are slight differences between the bone remodelling mechanism of capacitive and direct stimulations. Briefly, capacitive stimulation modulates bone formation and maturation through the activation of voltage-gated calcium channels, followed by the amplification of cytosolic calcium before boosting the intracellular calcium storage [44,129]. Concentrations of calmodulin, a mediator for proliferation and bone formation, are then activated to regulate bone healing processes by triggering osteoblastic growth factors, including bone morphogenetic protein (BMP) and transforming growth factor beta-1 (TGF-β1) [52,130]. The growth factors synthesised in direct stimulation, on the other hand, are mainly governed by BMP and vascular endothelial growth factor (VEGF) in association with increased pH and reduced oxygen levels [52,89]. The resultant hydroxyl ions produced from the redox reactions elevated the pH levels, and the secondary production of hydrogen peroxide (H_2O_2) activates bone formation through osteoclasts resorption [51,131]. In the present study, as no statistically significant difference on pH level and H_2O_2 concentration (Fig. 3b) were discovered in any of the experiment parameters as compared to the control group, one would hypothesise that the upregulation of calcium deposition levels was modulated by BMP and TGF-β1 osteoblastic growth factors. However, it was recognised that BMP coupled with VEGF could expedite bone regeneration and stem cells differentiation [132]; hence a further experiment could include the addition of VEGF growth factors, especially to 100 mV/mm group, to further induce the calcium mineralisation rate [89,133].

On the other hand, it is encouraging to notice that EF at a higher intensity (200 mV/mm) demonstrated early calcium mineralisation regardless of culture medium type. This finding is of major significance for the development of capacitive stimulation. Conventional culture medium with growth factors such as ascorbic acid and dexamethasone is widely employed in providing chemical cues to induce osteogenic responses in stem cells, but translating this practice into *in-vivo* settings is still far from ideal, because dexamethasone, for example, would cause systemic damage to animal tissues when used *in-vivo* [133]. Therefore, the utility of non-chemical methods in stem cell differentiation would prospectively provide an exciting opportunity to allow precise control of cellular behaviour with well-defined parameters and toxic-free approach in directing cell growth, directionality and stem cell differentiation. Additionally, this non-invasive electrotherapy approach would further benefit researchers in a variety of applications, such as wound healing [134], nerve regeneration, cardiovascular treatment, musculoskeletal rehabilitation, limb regeneration [135,136], and orthopaedic implant osseointegration [22].

3.5. Limitations and future work

Although the study has successfully demonstrated that the presence of capacitive stimulation regime incorporated with cp Ti discs has a positive impact on stem cell proliferation, orientation and bone mineralisation, it has certain limitations that need to be acknowledged. Firstly, the simulated EF used in this study was determined based on the finite element modelling data, and the validation of EF parameters was not feasible due to practical and technical constraints. Furthermore, the direct current power supply unit employed in this study was limited to a maximum potential of 30 V, hence an *in-vitro* investigation using higher EF intensity was not achievable, although it might be favourable to discover and comprehend the effect of higher intensity EF on cell cultured on cp Ti discs under our capacitive stimulation bioreactor.

A number of possible future studies using the same experimental set up are apparent in the following areas: (1) a wider study range of EF intensity to find out the upper permissible intensity on the stem cells with this capacitive stimulation bioreactor. With this, a maximum effect of ES will also provide a better understanding of the cell-stimuli interactions; (2) mathematical verification or physical validation of the simulated EF would offer a more accurate measurement and precise analysis; (3) extended experiment period to investigate long-term continuous capacitive stimulation on cellular responses; (4) the incorporation of more detailed *in-vitro* functional assays to study the cellular mechanism under the influence of capacitive ES regime, such as real-time polymerase chain reaction (RT-qPCR) for specific growth factors, and migration assay for wound healing applications; (5) the manipulation of different electrical modality in association with the capacitive stimulation to examine the effect of pulsatile, biphasic and multi-levelled frequency stimulation regimes on cellular behaviours [21,27,137]; (6) different biocompatible substrates with varied conductivity to explore the effect of substrate conductivity on stimulated cells [126,138]; and (7) *in-vitro* assessment with a variety of cell lineage, including a diversity of mammalian cells, phagocytes, bacterial species and viruses [139,140] to widen the range of application using this bioreactor.

4. Conclusion

Electrical Stimulation (ES) has been widely employed in a great number of research and clinical settings, including nerve regeneration, intervertebral rehabilitation, musculoskeletal and orthopaedic applications. With the use of the appropriate electric field, ES therapy evokes biochemical and physiological pathways that lead to effective and targeted healthcare treatment. This manuscript presents an imperative approach on combining cp Ti (primarily preferred as medical implant materials) and ES in a purpose-built bioreactor with capacitive stimulation delivery system. A continuous capacitive stimulation regime on titanium disc has resulted in enhanced cell proliferation rate of human mesenchymal stem cells with an elongated and differentiated morphology under the regime of 200 mV/mm on cp Ti discs, with evidence of nuclear elongation and cytoskeletal orientation perpendicular to the direction of electric field. As opposed to the commonly used direct stimulation regime, the capacitive stimulation were proven to be suitability for long-term toxic free stimulation as there were no pH fluctuations and hydrogen peroxide production caused by Faradic reactions. The increase in alkaline phosphatase production and calcium deposition observed on samples exposed to 200 mV/mm evidently

showed that early stem cell differentiation and matrix production were observed even without the presence of chemical osteoinductive growth factors.

This study showed the first time that the upregulation of stem cell function and commitment through capacitive stimulation in conjugation with MSCs cultured on cp Ti discs. The findings of this study have a number of important implications for future practice. As the capacitive stimulation bioreactor was able to evident the potential use in regenerative bone therapy, it can be translated with clinical relevance for further use in *in-vivo* animal tests, for which the stimulator design, with or without the titanium implant, could be further optimised and commercially viable in correlation to anatomical and physiological responses. In the event of successful use of this capacitive stimulation regime in implant integration and fracture rehabilitation with minimal inflammatory response, an ultimate translation of this bioreactor model into a wearable stimulation device would be possible to assist the unmet clinal need relating to limb regeneration, nerve rehabilitation, bone fracture treatment and wound healing electrotherapy.

Declaration of Competing Interest

The authors declare that there are no conflicts of interest regarding the publication of this paper.

Acknowledgements

The authors acknowledge the Engineering and Physical Sciences Research Council (grants EP/I02249X/1) for grant funding. Many thanks to colleagues in Cartmell group who provided a significant contribution to the research, including Sahba Mobini, Richard Balint, Andrea Fotticchia and Kasama Srirussami. The authors would like to express gratitude to fellow experimental officers and laboratory technicians, including Teruo Hashimoto, Louise Carney, Daniel Wilson and Gary Pickles, for their technical assistance and support.

References

[1] Zion Market Research, Dental Implants Market by Product (Endosteal Implants, Subperiosteal Implants, Transosteal Implants, and Intramucosal Implants), by Material (Titanium Implants and Zirconium Implants), and by End User (Hospitals, Dental Clinics, Academia, and Research Institutes): Global Industry Perspective, Comprehensive Analysis and Forecast, 2017 - 2024, New York, 2018. https://www.zionmarketresearch.com/news/dental-implants-market (accessed August 12, 2018).

[2] GlobalData Healthcare Intelligence Centre, Global orthopaedics market share value ($) in 2017, 2018. http://www.opnews.com/2018/05/global-orthopaedics-market-set-to-grow-to-66-2bn-by-2023/14548 (accessed August 12, 2018).

[3] , Titanium alloys for aerospace structures and engines, in: Introduction to Aerospace Materials, Elsevier, 2012, pp. 202–223, doi:10.1533/9780857095152.202.

[4] M. Munsch, Laser additive manufacturing of customized prosthetics and implants for biomedical applications, in: Laser Additive Manufacturing Materials, Design, Technologies, and Applications, Elsevier Inc., 2017, pp. 399–420, doi:10.1016/B978-0-08-100433-3.00015-4.

[5] M. Geetha, A.K. Singh, R. Asokamani, A.K. Gogia, Ti based biomaterials, the ultimate choice for orthopaedic implants – a review, Prog. Mater. Sci. 54 (2009) 397–425, doi:10.1016/J.PMATSCI.2008.06.004.

[6] V.S. de Viteri, E. Fuentes, Titanium and titanium alloys as biomaterials, Tribol. - Fundam. Adv., InTech, 2013, doi:10.5772/55860.

[7] A.T. Sidambe, Biocompatibility of advanced manufactured titanium implants—a review, Materials 7 (2014) 8168–8188, doi:10.3390/ma7128168.

[8] C.N. Elias, J.H.C. Lima, R. Valiev, M.A. Meyers, Biomedical applications of titanium and its alloys, JOM 60 (2008) 46–49, doi:10.1007/s11837-008-0031-1.

[9] Y. Oshida, Biosci. Bioeng. Titanium Mater. (2007), doi:10.1016/B978-008045142-8/50011-6.

[10] P. Bocchetta, L.Y. Chen, J.D.C. Tardelli, A.C. Dos Reis, F. Almeraya-Calderón, P. Leo, Passive layers and corrosion resistance of biomedical ti-6al-4v and β-ti alloys, Coatings 11 (2021) 11, doi:10.3390/coatings11050487.

[11] E. Fuentes, S. Alves, A. López-Ortega, L. Mendizabal, V. Sáenz de Viteri, Advanced surface treatments on titanium and titanium alloys focused on electrochemical and physical technologies for biomedical applications, Biomater. Tissue Reconstr. or Regen., IntechOpen, 2019, doi:10.5772/intechopen.85095.

[12] V. Huynh, N.K. Ngo, T.D. Golden, Surface activation and pretreatments for biocompatible metals and alloys used in biomedical applications, Int. J. Biomater. (2019) 2019, doi:10.1155/2019/3806504.

[13] L. Bins-Ely, K. Cesca, F.S. Souza, L. Porto, A. Spinelli, R. Magini, B. Henriques, J.C.M. Souza, On the increase of the chemical reactivity of cp titanium and Ti6Al4V at low electrical current in a protein-rich medium, Biomed. Phys. Eng. Express. 5 (2019) 015014, doi:10.1088/2057-1976/aae409.

[14] E.S. Ogawa, A.O. Matos, T. Beline, I.S.V. Marques, C. Sukotjo, M.T. Mathew, E.C. Rangel, N.C. Cruz, M.F. Mesquita, R.X. Consani, V.A.R. Barão, Surface-treated commercially pure titanium for biomedical applications: electrochemical, structural, mechanical and chemical characterizations, Mater. Sci. Eng. C 65 (2016) 251–261, doi:10.1016/J.MSEC.2016.04.036.

[15] B. Feng, X. Chu, J. Chen, J. Wang, X. Lu, J. Weng, Hydroxyapatite coating on titanium surface with titania nanotube layer and its bond strength to substrate, J. Porous Mater. 17 (2009) 453–458, doi:10.1007/s10934-009-9307-2.

[16] Y. Wang, C. Wen, P. Hodgson, Y. Li, Biocompatibility of TiO2 nanotubes with different topographies, J. Biomed. Mater. Res. A 102 (2014) 743–751, doi:10.1002/jbm.a.34738.

[17] M.J.P. Biggs, R.G. Richards, M.J. Dalby, Nanotopographical modification: a regulator of cellular function through focal adhesions, Nanomedicine 6 (2010) 619–633, doi:10.1016/j.nano.2010.01.009.

[18] T.K. Monsees, K. Barth, S. Tippelt, K. Heidel, A. Gorbunov, W. Pompe, R.H.W. Funk, Effects of different titanium alloys and nanosize surface patterning on adhesion, differentiation, and orientation of osteoblast-like cells, Cells Tissues Organs 180 (2005) 81–95, doi:10.1159/000086749.

[19] Y. Li, C. Yang, H. Zhao, S. Qu, X. Li, Y. Li, New developments of Ti-based alloys for biomedical applications, Materials 7 (2014) 1709–1800, doi:10.3390/ma7031709.

[20] G. Zacchetti, A. Wiskott, J. Cugnoni, J. Botsis, P. Ammann, External mechanical microstimuli modulate the osseointegration of titanium implants in rat tibiae, Biomed Res. Int. 2013 (2013) 234093, doi:10.1155/2013/234093.

[21] B. Ercan, T.J. Webster, The effect of biphasic electrical stimulation on osteoblast function at anodized nanotubular titanium surfaces, Biomaterials 31 (2010) 3684–3693, doi:10.1016/J.BIOMATERIALS.2010.01.078.

[22] P.R. Kuzyk, E.H. Schemitsch, The science of electrical stimulation therapy for fracture healing, Indian J. Orthop. 43 (2009) 127–131, doi:10.4103/0019-5413.50846.

[23] J.Behari Jayanand, Effect of electrical stimulation in mineralization and collagen enrichment of osteoporotic rat bones, in: 2008 International Conference on Recent Advances in Microwave Theory and Applications, IEEE, 2008, pp. 568–571, doi:10.1109/AMTA.2008.4763231.

[24] R. Balint, N.J. Cassidy, S.H. Cartmell, Electrical stimulation: a novel tool for tissue engineering, Tissue Eng. Part B Rev. 19 (2013) 48–57, doi:10.1089/ten.teb.2012.0183.

[25] C.T. Brighton, S.R. Pollack, Treatment of recalcitrant non-union with a capacitively coupled electrical field. A preliminary report, J. Bone Jt. Surg. Am. 67 (1985) 577–585 http://www.ncbi.nlm.nih.gov/pubmed/3872300 (accessed May 20, 2018).

[26] B. Bisceglia, A. De Vita, M. Sarti, Numeric simulation of a therapeutic processing, COMPEL – Int. J. Comput. Math. Electr. Electron. Eng. 27 (2008) 1249–1259, doi:10.1108/03321640810905738.

[27] D. Hernández Vaquero, C. Hernández-Vaquero Panizo, The effect of electromagnetic stimulation on nonunions: myth or reality? Rev. Española Cirugía Ortopédica y Traumatol. 51 (2007) 354–362, doi:10.1016/S1988-8856(07)70057-3.

[28] R.A. Gittens, R. Olivares-Navarrete, R. Tannenbaum, B.D. Boyan, Z. Schwartz, Electrical implications of corrosion for osseointegration of titanium implants, J. Dent. Res. 90 (2011) 1389–1397, doi:10.1177/0022034511408428.

[29] M.N. Hirt, J. Boeddinghaus, A. Mitchell, S. Schaaf, C. Börnchen, C. Müller, H. Schulz, N. Hubner, J. Stenzig, A. Stoehr, C. Neuber, A. Eder, P.K. Luther, A. Hansen, T. Eschenhagen, Functional improvement and maturation of rat and human engineered heart tissue by chronic electrical stimulation, J. Mol. Cell. Cardiol. 74 (2014) 151–161, doi:10.1016/j.yjmcc.2014.05.009.

[30] N. Tandon, B. Goh, A. Marsano, P.-H.G. Chao, C. Montouri-Sorrentino, J. Gimble, G. Vunjak-Novakovic, Alignment and elongation of human adipose-derived stem cells in response to direct-current electrical stimulation, in: 2009 Annual International Conference of the IEEE Engineering in Medicine and Biology Society, IEEE, 2009, pp. 6517–6521, doi:10.1109/IEMBS.2009.5333142.

[31] L. Bins-Ely, D. Suzuki, R. Magini, C.A.M. Benfatti, W. Teughels, B. Henriques, J.C.M. Souza, Enhancing the bone healing on electrical stimuli through the dental implant, Comput. Methods Biomech. Biomed. Eng. 23 (2020) 1041–1051, doi:10.1080/10255842.2020.1785437.

[32] L.M. Bins-Ely, E.B. Cordero, J.C.M. Souza, W. Teughels, C.A.M. Benfatti, R.S. Magini, *In vivo* electrical application on titanium implants stimulating bone formation, J. Periodontal Res. 52 (2017) 479–484, doi:10.1111/jre.12413.

[33] Y.-S. Sun, Electrical stimulation for wound-healing: simulation on the effect of electrode configurations, Biomed Res. Int. 2017 (2017) 1–9, doi:10.1155/2017/5289041.

[34] S. Ud-Din, A. Sebastian, P. Giddings, J. Colthurst, S. Whiteside, J. Morris, R. Nuccitelli, C. Pullar, M. Baguneid, A. Bayat, Angiogenesis is induced and wound size is reduced by electrical stimulation in an acute wound healing model in human skin, PLoS One 10 (2015) e0124502, doi:10.1371/journal.pone.0124502.

[35] L.C. Kloth, Electrical stimulation technologies for wound healing, Adv. Wound Care 3 (2014) 81–90, doi:10.1089/wound.2013.0459.

[36] G. Thakral, J. Lafontaine, B. Najafi, T.K. Talal, P. Kim, L.A. Lavery, Electrical stimulation to accelerate wound healing, Diabet. Foot Ankle 4 (2013), doi:10.3402/dfa.v4i0.22081.
[37] H.J. Park, M. Rouabhia, D. Lavertu, Z. Zhang, Electrical stimulation modulates the expression of multiple wound healing genes in primary human dermal fibroblasts, Tissue Eng. Part A. 21 (2015) 1982–1990, doi:10.1089/ten.tea.2014.0687.
[38] P.M. Rossini, D. Burke, R. Chen, L.G. Cohen, Z. Daskalakis, R. Di Iorio, V. Di Lazzaro, F. Ferreri, P.B. Fitzgerald, M.S. George, M. Hallett, J.P. Lefaucheur, B. Langguth, H. Matsumoto, C. Miniussi, M.A. Nitsche, A. Pascual-Leone, W. Paulus, S. Rossi, J.C. Rothwell, H.R. Siebner, Y. Ugawa, V. Walsh, U. Ziemann, Non-invasive electrical and magnetic stimulation of the brain, spinal cord, roots and peripheral nerves: Basic principles and procedures for routine clinical and research application. An updated report from an I.F.C.N. Committee, Clin. Neurophysiol. 126 (2015) 1071–1107, doi:10.1016/J.CLINPH.2015.02.001.
[39] R.A. McBain, C.L. Boswell-Ruys, B.B. Lee, S.C. Gandevia, J.E. Butler, Electrical stimulation of abdominal muscles to produce cough in spinal cord injury, Neurorehabil. Neural Repair. 29 (2015) 362–369, doi:10.1177/1545968314552527.
[40] G. Deley, J. Denuziller, N. Babault, J.A. Taylor, Effects of electrical stimulation pattern on quadriceps isometric force and fatigue in individuals with spinal cord injury, Muscle Nerve 52 (2015) 260–264, doi:10.1002/mus.24530.
[41] E. Krueger, L. Magri, A. Botelho, F. Bach, C. Rebelatto, L. Fracaro, F. Fragoso, J.V. JR, P. Brofman, L. Popovic-Maneski, Low-intensity electrical stimulation and stem cells in a dog with acute spinal cord injury, Biomed. Eng. (NY)., ACTAPRESS, 2017, doi:10.2316/P.2017.852-007.
[42] C.H. Ho, R.J. Triolo, A.L. Elias, K.L. Kilgore, A.F. DiMarco, K. Bogie, A.H. Vette, M.L. Audu, R. Kobetic, S.R. Chang, K.M. Chan, S. Dukelow, D.J. Bourbeau, S.W. Brose, K.J. Gustafson, Z.H.T. Kiss, V.K. Mushahwar, Functional electrical stimulation and spinal cord injury, Phys. Med. Rehabil. Clin. N. Am. 25 (2014) 631–654 ix, doi:10.1016/j.pmr.2014.05.001.
[43] S. Hamid, R. Hayek, Role of electrical stimulation for rehabilitation and regeneration after spinal cord injury: an overview, Eur. Spine J. 17 (2008) 1256–1269, doi:10.1007/s00586-008-0729-3.
[44] C.T. Brighton, W. Wang, R. Seldes, G. Zhang, S.R. Pollack, Signal transduction in electrically stimulated bone cells, J. Bone Jt. Surg. Am. 83-A (2001) 1514–1523 http://www.ncbi.nlm.nih.gov/pubmed/11679602 (accessed January 17, 2018).
[45] T.-K. Wong, E. Neumann, Electric field mediated gene transfer, Biochem. Biophys. Res. Commun. 107 (1982) 584–587, doi:10.1016/0006-291X(82)91531-5.
[46] C.-Y. Su, T. Fang, H.-W. Fang, Effects of electrostatic field on osteoblast cells for bone regeneration applications, Biomed Res. Int. 2017 (2017) 7124817, doi:10.1155/2017/7124817.
[47] T.A. Banks, P.S.B. Luckman, J.E. Frith, J.J. Cooper-White, Effects of electric fields on human mesenchymal stem cell behaviour and morphology using a novel multichannel device, Integr. Biol. 7 (2015) 693–712, doi:10.1039/C4IB00297K.
[48] J.P. Woock, P.B. Yoo, W.M. Grill, Finite element modeling and in vivo analysis of electrode configurations for selective stimulation of pudendal afferent fibers, BMC Urol 10 (2010) http://www.biomedcentral.com/1471-2490/10/11 (accessed May 20, 2018).
[49] C.C. McIntyre, W.M. Grill, Finite element analysis of the current-density and electric field generated by metal microelectrodes, Ann. Biomed. Eng. 29 (2001) 227–235, doi:10.1114/1.1352640.
[50] A. Patriciu, T.P. DeMonte, M.L.G. Joy, J.J. Struijk, Investigation of current densities produced by surface electrodes using finite element modeling and current density imaging, in: 2001 Conference Proceedings of the 23rd Annual International Conference of the IEEE Engineering in Medicine and Biology Society, IEEE, 2001, pp. 2403–2406, doi:10.1109/IEMBS.2001.1017261.
[51] M. Griffin, A. Bayat, Electrical stimulation in bone healing: critical analysis by evaluating levels of evidence, J. Plast. Surg. (2011) http://www.eplasty.com/images/PDF/eplasty11e34.pdf (accessed May 17, 2018).
[52] J.C. Gan, D.C. Fredericks, P.A. Glazer, Direct current and capacitive coupling electrical stimulation upregulates osteopromotive factors for spinal fusions, in: Conference Proceeding, 2005 https://www.pdfs.semanticscholar.org/1f10/876a719d22797b3b3af432da50abd78f3691.pdf?_ga=2.157546110.551344279.1526514976-1948264527.1526514976 (accessed May 17, 2018).
[53] T. Shigino, M. Ochi, H. Kagami, K. Sakaguchi, O. Nakade, Application of capacitively coupled electric field enhances periimplant osteogenesis in the dog mandible, Int. J. Prosthodont. 13 (2000) 365–372 http://www.ncbi.nlm.nih.gov/pubmed/11203655 (accessed May 20, 2018).
[54] Z. Wang, W.C. Hutton, S.T. Yoon, The effect of capacitively coupled (CC) electrical stimulation on human disc nucleus pulposus cells and the relationship between CC and BMP-7, Eur. Spine J. 26 (2017) 240–247, doi:10.1007/s00586-016-4439-y.
[55] G. Thrivikraman, S.K. Boda, B. Basu, Unraveling the mechanistic effects of electric field stimulation towards directing stem cell fate and function: a tissue engineering perspective, Biomaterials 150 (2018) 60–86, doi:10.1016/J.BIOMATERIALS.2017.10.003.
[56] B. Ercan, T.J. Webster, Greater osteoblast proliferation on anodized nanotubular titanium upon electrical stimulation, Int. J. Nanomed. 3 (2008) 477–485 https://www.ncbi.nlm.nih.gov/pmc/articles/PMC2636582/pdf/IJN-3-477.pdf (accessed December 19, 2017).
[57] B. Ercan, K.M. Kummer, K.M. Tarquinio, T.J. Webster, Decreased Staphylococcus aureus biofilm growth on anodized nanotubular titanium and the effect of electrical stimulation, Acta Biomater. 7 (2011) 3003–3012, doi:10.1016/J.ACTBIO.2011.04.002.
[58] C.N. Elias, D.J. Fernandes, F.M. De Souza, E.D.S. Monteiro, R.S. De Biasi, Mechanical and clinical properties of titanium and titanium-based alloys (Ti G2, Ti G4 cold worked nanostructured and Ti G5) for biomedical applications, J. Mater. Res. Technol. 8 (2019) 1060–1069, doi:10.1016/j.jmrt.2018.07.016.
[59] A. Kuhn, T. Keller, M.L. Ae, M. Morari, A. Kuhn, Á.T. Keller, Á.M. Lawrence, Á.M. Morari, T. Keller, A model for transcutaneous current stimulation: simulations and experiments, Med. Biol. Eng. Comput. 47 (2009) 279–289, doi:10.1007/s11517-008-0422-z.
[60] M. Ito, D. Setoyama, J. Matsunaga, H. Muta, K. Kurosaki, M. Uno, S. Yamanaka, Electrical and thermal properties of titanium hydrides, J. Alloy. Compd. 420 (2006) 25–28, doi:10.1016/J.JALLCOM.2005.10.032.
[61] K. Srirussamee, R. Xue, S. Mobini, N.J. Cassidy, S.H. Cartmell, Changes in the extracellular microenvironment and osteogenic responses of mesenchymal stem/stromal cells induced by in vitro direct electrical stimulation, J. Tissue Eng. 12 (2021), doi:10.1177/2041731420974147.
[62] K. Srirussamee, S. Mobini, N.J. Cassidy, S.H. Cartmell, Direct electrical stimulation enhances osteogenesis by inducing Bmp2 and Spp1 expressions from macrophages and preosteoblasts, Biotechnol. Bioeng. 116 (2019) 3421–3432, doi:10.1002/bit.27142.
[63] R. Balint, N. Cassidy, S. Cartmell, Capacitive stimulation enhanced osteogenic differentiation of primary human mesenchymal stem cells, (2012) 332–332. https://www.research.manchester.ac.uk/portal/en/publications/capacitive-stimulation-enhanced-osteogenic-differentiation-of-primary-human-mesenchymal-stem-cells(b5ca1fcf-69af-44b4-a721-555d94f84d05)/export.html (accessed June 28, 2021).
[64] J.V. Hughes, H.L. Armstrong, The dielectric constant of dry air, J. Appl. Phys. 23 (1952) 501–504, doi:10.1063/1.1702240.
[65] M. Lorenzetti, E. Gongadze, M. Kulkarni, I. Junkar, A. Iglič, Electrokinetic properties of TiO2 nanotubular surfaces, Nanoscale Res. Lett. 11 (2016) 1–13, doi:10.1186/s11671-016-1594-3.
[66] A. Apolinário, C.T. Sousa, J. Ventura, J.D. Costa, D.C. Leitão, J.M. Moreira, J.B. Sousa, L. Andrade, A.M. Mendes, J.P. Araújo, The role of the Ti surface roughness on the self-ordering of TiO2 nanotubes: a detailed study of the growth mechanism, J. Mat.Chem. (2014) 1–3 00, doi:10.1039/x0xx00000x.
[67] J.A. Ryan, Use of Corning ® Cloning Cylinders for Harvesting Cell Colonies, New York, 2003 https://www.fishersci.co.uk/content/dam/fishersci/en_EU/suppliers/corning/cc_cloning_protocol_1_03_cls_an_041w.pdf (accessed November 7, 2018).
[68] J.S. Khaw, C.R. Bowen, S.H. Cartmell, Effect of TiO2 nanotube pore diameter on human mesenchymal stem cells and human osteoblasts, Nanomaterials 10 (2020) 2117, doi:10.3390/nano10112117.
[69] S. Goldenthal, Bilateral and unilateral activation of the diaphragm in the intact human. External electrical stimulation by capacitive coupling as recorded by cineradiography, Conn. Med. 25 (1961) 236–238 http://www.ncbi.nlm.nih.gov/pubmed/13706500 (accessed May 20, 2018).
[70] C.T. Brighton, G.B. Pfeffer, S.R. Pollack, In vivo growth plate stimulation in various capacitively coupled electrical fields, J. Orthop. Res. 1 (1983) 42–49, doi:10.1002/jor.1100010106.
[71] S. Ment, Effects of Seven Days of Continuous Capacitive Electrical Stimulation on Bone Growth Around Titanium Implants in the Rat Tibia, McGill, 1999 http://digitool.library.mcgill.ca/R/?func=dbin-jump-full&object_id=30703&local_base=GEN01-MCG02 (accessed December 24, 2018).
[72] C.B. Goodwin, C.T. Brighton, R.D. Guyer, J.R. Johnson, K.I. Light, H.A. Yuan, A double-blind study of capacitively coupled electrical stimulation as an adjunct to lumbar spinal fusions., Spine (Phila. Pa. 1976) 24 (1999) 1349–1356 discussion 1357. http://www.ncbi.nlm.nih.gov/pubmed/10404578 (accessed December 24, 2018).
[73] P. Zamora-Navas, A. Borras Verdera, R. Antelo Lorenzo, J.R. Saras Ayuso, M.C. Peña Reina, Electrical stimulation of bone nonunion with the presence of a gap, Acta Orthop. Belg. 61 (1995) 169–176 http://www.ncbi.nlm.nih.gov/pubmed/8525812 (accessed May 20, 2018).
[74] R.I. Abeed, M. Naseer, E.W. Abel, Capacitively coupled electrical stimulation treatment: results from patients with failed long bone fracture unions, J. Orthop. Trauma 12 (1998) 510–513 https://insights.ovid.com/pubmed?pmid=9781776 (accessed May 20, 2018).
[75] C.T. Brighton, E. Okereke, S.R. Pollack, C.C. Clark, In vitro bone-cell response to a capacitively coupled electrical field. The role of field strength, pulse pattern, and duty cycle, Clin. Orthop. Relat. Res. (1992) 255–262 http://www.ncbi.nlm.nih.gov/pubmed/1446447 (accessed December 24, 2018).
[76] H. Ye, A. Steiger, Neuron matters: electric activation of neuronal tissue is dependent on the interaction between the neuron and the electric field, J. Neuroeng. Rehabil. 12 (2015) 65, doi:10.1186/s12984-015-0061-1.
[77] D.R. Merrill, M. Bikson, J.G.R. Jefferys, Electrical stimulation of excitable tissue: design of efficacious and safe protocols, J. Neurosci. Methods 141 (2005) 171–198, doi:10.1016/J.JNEUMETH.2004.10.020.
[78] Y. Yang, W. Gao, Wearable and flexible electronics for continuous molecular monitoring, Chem. Soc. Rev. (2019), doi:10.1039/C7CS00730B.
[79] D. Giovanelli, E. Farella, Force sensing resistor and evaluation of technology for wearable body pressure sensing, J. Sens. 2016 (2016) 1–13, doi:10.1155/2016/9391850.

[80] M.S. Brown, B. Ashley, A. Koh, Wearable technology for chronic wound monitoring: current dressings, advancements, and future prospects, Front. Bioeng. Biotechnol. 6 (2018) 47, doi:10.3389/fbioe.2018.00047.
[81] K.-A. Chang, J.W. Kim, J. a Kim, S. Lee, S. Kim, W.H. Suh, H.-S. Kim, S. Kwon, S.J. Kim, Y.-H. Suh, Biphasic electrical currents stimulation promotes both proliferation and differentiation of fetal neural stem cells, PLoS One 6 (2011) e18738, doi:10.1371/journal.pone.0018738.
[82] F. Qi, Y. Wang, T. Ma, S. Zhu, W. Zeng, X. Hu, Z. Liu, J. Huang, Z. Luo, Electrical regulation of olfactory ensheathing cells using conductive polypyrrole/chitosan polymers, Biomaterials 34 (2013) 1799–1809, doi:10.1016/j.biomaterials.2012.11.042.
[83] E. Mooney, J.N. Mackle, D.J-P Blond, G. Shaw, W.J. Blau, F.P. Barry, V. Barron, J. Mary Murphy, The electrical stimulation of carbon nanotubes to provide a cardiomimetic cue to MSCs, Biomaterials 33 (2012) 6132–6139, doi:10.1016/j.biomaterials.2012.05.032.
[84] M. Canillas, B. Moreno, E. Chinarro, A.M. Rajnicek, TiO 2 surfaces support neuron growth during electric field stimulation, Mater. Sci. Eng. C 79 (2017) 1–8, doi:10.1016/j.msec.2017.04.135.
[85] H. Bai, J.V. Forrester, M. Zhao, DC electric stimulation upregulates angiogenic factors in endothelial cells through activation of VEGF receptors, Cytokine 55 (2011) 110–115, doi:10.1016/J.CYTO.2011.03.003.
[86] P. Petrov, P. Mokreva, I. Kostov, V. Uzunova, R. Tzoneva, Novel electrically conducting 2-hydroxyethylcellulose/polyaniline nanocomposite cryogels: synthesis and application in tissue engineering, Carbohydr. Polym. 140 (2016) 349–355, doi:10.1016/j.carbpol.2015.12.069.
[87] W.-W. Hu, Y.-T. Hsu, Y.-C. Cheng, C. Li, R.-C. Ruaan, C.-C. Chien, C.-A. Chung, C.-W. Tsao, Electrical stimulation to promote osteogenesis using conductive polypyrrole films, Mater. Sci. Eng. C. 37 (2014) 28–36, doi:10.1016/J.MSEC.2013.12.019.
[88] Z. Liu, L. Dong, L. Wang, X. Wang, K. Cheng, Z. Luo, W. Weng, Mediation of cellular osteogenic differentiation through daily stimulation time based on polypyrrole planar electrodes, Sci. Rep. 7 (2017) 17926, doi:10.1038/s41598-017-17120-8.
[89] I.S. Kim, J.K. Song, Y.L. Zhang, T.H. Lee, T.H. Cho, Y.M. Song, D.K. Kim, S.J. Kim, S.J. Hwang, Biphasic electric current stimulates proliferation and induces VEGF production in osteoblasts, Biochim. Biophys. Acta – Mol. Cell Res. 1763 (2006) 907–916, doi:10.1016/J.BBAMCR.2006.06.007.
[90] R.J. Fitzsimmons, J. Farley, W.R. Adey, D.J. Baylink, Embryonic bone matrix formation is increased after exposure to a low-amplitude capacitively coupled electric field, in vitro, Biochim. Biophys. Acta – Gen. Subj. 882 (1986) 51–56, doi:10.1016/0304-4165(86)90054-1.
[91] M. Hartig, U. Joos, H.-P. Wiesmann, Capacitively coupled electric fields accelerate proliferation of osteoblast-like primary cells and increase bone extracellular matrix formation in vitro, Eur. Biophys. J. 29 (2000) 499–506, doi:10.1007/s002490000100.
[92] C. Oldani, A. Dominguez, Titanium as a biomaterial for implants, Recent Adv. Arthroplast., InTech, 2012, doi:10.5772/27413.
[93] L. Kyllönen, S. Haimi, B. Mannerström, H. Huhtala, K.M. Rajala, H. Skottman, G.K. Sándor, S. Miettinen, Effects of different serum conditions on osteogenic differentiation of human adipose stem cells in vitro, Stem Cell Res. Ther. 4 (2013) 17, doi:10.1186/scrt165.
[94] L. Tirkkonen, S. Haimi, S. Huttunen, J. Wolff, E. Pirhonen, G.K. Sándor, S. Miettinen, Osteogenic medium is superior to growth factors in differentiation of human adipose stem cells towards bone-forming cells in 3D culture, Eur. Cell. Mater. 25 (2013) 144–158 http://www.ncbi.nlm.nih.gov/pubmed/23361609 (accessed December 27, 2018).
[95] P. Sanjuan-Alberte, M.R. Alexander, R.J.M. Hague, F.J. Rawson, Electrochemically stimulating developments in bioelectronic medicine, Bioelectron. Med. 4 (2018) 1, doi:10.1186/s42234-018-0001-z.
[96] H. -y. Yang, R.-P. Charles, E. Hummler, D.L. Baines, R.R. Isseroff, The epithelial sodium channel mediates the directionality of galvanotaxis in human keratinocytes, J. Cell Sci. 126 (2013) 1942–1951, doi:10.1242/jcs.113225.
[97] S.N. Iwasa, R. Babona-Pilipos, C.M. Morshead, Environmental factors that influence stem cell migration: an "Electric Field, Stem Cells Int 2017 (2017) 1–9, doi:10.1155/2017/4276927.
[98] K. Nakajima, K. Zhu, Y.-H. Sun, B. Hegyi, Q. Zeng, C.J. Murphy, J.V. Small, Y. Chen-Izu, Y. Izumiya, J.M. Penninger, M. Zhao, KCNJ15/Kir4.2 couples with polyamines to sense weak extracellular electric fields in galvanotaxis, Nat. Commun. 6 (2015) 8532, doi:10.1038/ncomms9532.
[99] T. Gordonov, E. Kim, Y. Cheng, H. Ben-Yoav, R. Ghodssi, G. Rubloff, J.-J. Yin, G.F. Payne, W.E. Bentley, Electronic modulation of biochemical signal generation, Nat. Nanotechnol. 9 (2014) 605–610, doi:10.1038/nnano.2014.151.
[100] S. Zhu, W. Jing, X. Hu, Z. Huang, Q. Cai, Y. Ao, X. Yang, Time-dependent effect of electrical stimulation on osteogenic differentiation of bone mesenchymal stromal cells cultured on conductive nanofibers, J. Biomed. Mater. Res. Part A 105 (2017) 3369–3383, doi:10.1002/jbm.a.36181.
[101] A. Kotwal, C.E. Schmidt, Electrical stimulation alters protein adsorption and nerve cell interactions with electrically conducting biomaterials, Biomaterials 22 (2001) 1055–1064, doi:10.1016/S0142-9612(00)00344-6.
[102] F. Pires, Q. Ferreira, C.A.V. Rodrigues, J. Morgado, F.C. Ferreira, Neural stem cell differentiation by electrical stimulation using a cross-linked PEDOT substrate: Expanding the use of biocompatible conjugated conductive polymers for neural tissue engineering, Biochim. Biophys. Acta – Gen. Subj. 1850 (2015) 1158–1168, doi:10.1016/J.BBAGEN.2015.01.020.
[103] M. Versaevel, T. Grevesse, S. Gabriele, Regulation of nuclear shape and function with cell elongation, Biophys. J. 104 (2013) 151a, doi:10.1016/j.bpj.2012.11.856.
[104] B. Chen, C. Co, C.-C. Ho, Cell shape dependent regulation of nuclear morphology, Biomaterials 67 (2015) 129–136, doi:10.1016/j.biomaterials.2015.07.017.
[105] X. Yao, R. Peng, J. Ding, Effects of aspect ratios of stem cells on lineage commitments with and without induction media, Biomaterials 34 (2013) 930–939, doi:10.1016/J.BIOMATERIALS.2012.10.052.
[106] M. Zhao, H. Bai, E. Wang, J.V Forrester, C.D. McCaig, Electrical stimulation directly induces pre-angiogenic responses in vascular endothelial cells by signaling through VEGF receptors, J. Cell Sci. 117 (2004) 397–405, doi:10.1242/jcs.00868.
[107] C. Lo Sicco, R. Tasso, Harnessing endogenous cellular mechanisms for bone repair, Front. Bioeng. Biotechnol. 5 (2017) 52, doi:10.3389/fbioe.2017.00052.
[108] R. Hunt, A. Zavalin, A. Bhatnagar, S. Chinnasamy, K. Das, Electromagnetic biostimulation of living cultures for biotechnology, biofuel and bioenergy applications, Int. J. Mol. Sci. 10 (2009) 4515–4558, doi:10.3390/ijms10104515.
[109] M. Mendoza, Influence and Effects of Dc Electric Fields on Bone Cells, Ruhr-Universität Bochum, 2003 http://www-brs.ub.ruhr-uni-bochum.de/netahtml/HSS/Diss/MironMendozaMiguel/diss.pdf (accessed November 2, 2018).
[110] S. Pietronave, A. Zamperone, F. Oltolina, D. Colangelo, A. Follenzi, E. Novelli, M. Diena, A. Pavesi, F. Consolo, G.B. Fiore, M. Soncini, M. Prat, Monophasic and biphasic electrical stimulation induces a precardiac differentiation in progenitor cells isolated from human heart, Stem Cells Dev. 23 (2014) 888–898, doi:10.1089/scd.2013.0375.
[111] M. Zhao, A. Agius-Fernandez, J.V Forrester, C.D. McCaig, Orientation and directed migration of cultured corneal epithelial cells in small electric fields are serum dependent, J. Cell Sci. 109 (Pt 6) (1996) 1405–1414 http://www.ncbi.nlm.nih.gov/pubmed/8799828 (accessed December 27, 2018).
[112] H.-F. Tsai, J.-Y. Cheng, H.-F. Chang, T. Yamamoto, A.Q. Shen, Uniform electric field generation in circular multi-well culture plates using polymeric inserts, Sci. Rep. 6 (2016) 26222, doi:10.1038/srep26222.
[113] K.R. Robinson, The responses of cells to electrical fields: a review, J. Cell Biol. 101 (1985) 2023–2027 http://www.ncbi.nlm.nih.gov/pubmed/3905820 (accessed December 27, 2018).
[114] M.S. Cooper, R.E. Keller, Perpendicular orientation and directional migration of amphibian neural crest cells in dc electrical fields, Proc. Natl. Acad. Sci. USA 81 (1984) 160–164 http://www.ncbi.nlm.nih.gov/pubmed/6582473 (accessed December 27, 2018).
[115] K.Y. Nishimura, R.R. Isseroff, R. Nuccitelli, Human keratinocytes migrate to the negative pole in direct current electric fields comparable to those measured in mammalian wounds, J. Cell Sci. 109 (Pt 1) (1996) 199–207 http://www.ncbi.nlm.nih.gov/pubmed/8834804 (accessed December 27, 2018).
[116] H. Zhang, M. Labouesse, Signalling through mechanical inputs – a coordinated process, J. Cell Sci. 125 (2012) 3039–3049, doi:10.1242/jcs.093666.
[117] M.A. Basson, Signaling in cell differentiation and morphogenesis, Cold Spring Harb. Perspect. Biol. 4 (2012), doi:10.1101/cshperspect.a008151.
[118] B. Cortese, I.E. Palamà, S. D'Amone, G. Gigli, Influence of electrotaxis on cell behaviour, Integr. Biol. 6 (2014) 817–830, doi:10.1039/c4ib00142g.
[119] J.-M. Lee, M.-G. Kim, J.-H. Byun, G.-C. Kim, J.-H. Ro, D.-S. Hwang, B.-B. Choi, G.-C. Park, U.-K. Kim, The effect of biomechanical stimulation on osteoblast differentiation of human jaw periosteum-derived stem cells, Maxillofac. Plast. Reconstr. Surg. 39 (2017) 7, doi:10.1186/s40902-017-0104-6.
[120] E. Castrén, T. Sillat, S. Oja, A. Noro, A. Laitinen, Y.T. Konttinen, P. Lehenkari, M. Hukkanen, M. Korhonen, Osteogenic differentiation of mesenchymal stromal cells in two-dimensional and three-dimensional cultures without animal serum, Stem Cell Res. Ther. 6 (2015) 167, doi:10.1186/s13287-015-0162-6.
[121] E.E. Golub, K. Boesze-Battaglia, The role of alkaline phosphatase in mineralization, Curr. Opin. Orthop. 18 (2007) 444–448, doi:10.1097/BCO.0b013e3282630851.
[122] H. Paul, A.J. Reginato, H.R. Schumacher, Alizarin red S staining as a screening test to detect calcium compounds in synovial fluid, Arthritis Rheum. 26 (1983) 191–200 http://www.ncbi.nlm.nih.gov/pubmed/6186260 (accessed December 28, 2018).
[123] J. Davies, Tissue Regeneration – From Basic Biology to Clinical Application, InTech, 2012, doi:10.5772/1334.
[124] G. Thrivikraman, P.S. Lee, R. Hess, V. Haenchen, B. Basu, D. Scharnweber, Interplay of substrate conductivity, cellular microenvironment, and pulsatile electrical stimulation toward osteogenesis of human mesenchymal stem cells in vitro, ACS Appl. Mater. Interfaces 7 (2015) 23015–23028, doi:10.1021/acsami.5b06390.
[125] J.G. Gershovich, R.L. Dahlin, F.K. Kasper, A.G. Mikos, Enhanced osteogenesis in cocultures with human mesenchymal stem cells and endothelial cells on polymeric microfiber scaffolds, Tissue Eng. Part A 19 (2013) 2565–2576, doi:10.1089/ten.TEA.2013.0256.
[126] A.S. Rowlands, J.J. Cooper-White, Directing phenotype of vascular smooth muscle cells using electrically stimulated conducting polymer, Biomaterials 29 (2008) 4510–4520, doi:10.1016/J.BIOMATERIALS.2008.07.052.
[127] B.L. Langdahl, M. Kassem, M.K. Møller, E.F. Eriksen, The effects of IGF-I and IGF-II on proliferation and differentiation of human osteoblasts and interactions with growth hormone, Eur. J. Clin. Investig. 28 (1998) 176–183 http://www.ncbi.nlm.nih.gov/pubmed/9568461 (accessed December 28, 2018).

[128] H. Zeng, J. Du, Q. Zheng, D. Duan, Y. Liu, A. Xiong, B. Kang, G. Liu, Effects of basic fibroblast growth factor on biological characteristics of osteoblasts, Chinese J. Traumatol. = Zhonghua Chuang Shang Za Zhi. 6 (2003) 229–233 http://www.ncbi.nlm.nih.gov/pubmed/12857517 (accessed December 28, 2018).
[129] S. Meng, M. Rouabhia, Z. Zhang, Electrical stimulation in tissue regeneration, Appl. Biomed. Eng., InTech, 2011, doi:10.5772/18874.
[130] C.C. Clark, W. Wang, C.T. Brighton, Up-regulation of expression of selected genes in human bone cells with specific capacitively coupled electric fields, J. Orthop. Res. 32 (2014) 894–903, doi:10.1002/jor.22595.
[131] L.M. Bins-Ely, E.B. Cordero, J.C.M. Souza, W. Teughels, C.A.M. Benfatti, R.S. Magini, In vivo electrical application on titanium implants stimulating bone formation, J. Periodontal Res. 52 (2017) 479–484, doi:10.1111/jre.12413.
[132] W. Zhang, C. Zhu, Y. Wu, D. Ye, S. Wang, D. Zou, X. Zhang, D.L. Kaplan, X. Jiang, VEGF and BMP-2 promote bone regeneration by facilitating bone marrow stem cell homing and differentiation, Eur. Cell. Mater. 27 (2014) 1–11 discussion 11-2. http://www.ncbi.nlm.nih.gov/pubmed/24425156 (accessed December 28, 2018).
[133] S.D. Eswaramoorthy, S. Bethapudi, S.I. Almelkar, S.N. Rath, Regional differentiation of adipose-derived stem cells proves the role of constant electric potential in enhancing bone healing, J. Med. Biol. Eng. 38 (2018) 804–815, doi:10.1007/s40846-018-0373-2.
[134] J. Hunckler, A. de Mel, A current affair: electrotherapy in wound healing, J. Multidiscip. Healthc. 10 (2017) 179–194, doi:10.2147/JMDH.S127207.
[135] L.P. Leppik, D. Froemel, A. Slavici, Z.N. Ovadia, L. Hudak, D. Henrich, I. Marzi, J.H. Barker, Effects of electrical stimulation on rat limb regeneration, a new look at an old model, Sci. Rep. 5 (2016) 18353, doi:10.1038/srep18353.
[136] R.O. Becker, J.A. Spadaro, Electrical stimulation of partial limb regeneration in mammals, Bull. N. Y. Acad. Med. 48 (1972) 627–641 http://www.ncbi.nlm.nih.gov/pubmed/4503923 (accessed December 17, 2018).
[137] H.T.H. Au, I. Cheng, M.F. Chowdhury, M. Radisic, Interactive effects of surface topography and pulsatile electrical field stimulation on orientation and elongation of fibroblasts and cardiomyocytes, Biomaterials 28 (2007) 4277–4293, doi:10.1016/J.BIOMATERIALS.2007.06.001.
[138] O. Akhavan, E. Ghaderi, S.A. Shirazian, R. Rahighi, Rolled graphene oxide foams as three-dimensional scaffolds for growth of neural fibers using electrical stimulation of stem cells, Carbon N. Y. 97 (2016) 71–77, doi:10.1016/J.CARBON.2015.06.079.
[139] H.L. Merriman, C.A. Hegyi, C.R. Albright-Overton, J. Carlos, R.W. Putnam, J.A. Mulcare, A comparison of four electrical stimulation types on Staphylococcus aureus growth in vitro, J. Rehabil. Res. Dev. 41 (2004) 139–146 http://www.ncbi.nlm.nih.gov/pubmed/15558368 (accessed January 4, 2019).
[140] K.C. Popat, M. Eltgroth, T.J. LaTempa, C.A. Grimes, T.A. Desai, Decreased Staphylococcus epidermis adhesion and increased osteoblast functionality on antibiotic-loaded titania nanotubes, Biomaterials 28 (2007) 4880–4888, doi:10.1016/J.BIOMATERIALS.2007.07.037.